ARTICLE 20

Excited electron: Pepliz LAN Empire II: LAN(P65) vs. LAN(P50) and ionization energy from Riquelme de Gozy

Javier Silvestre www.eeatom.blogspot.com

ABSTRACT

This is 20th article of 24 dedicated to atomic model based on Victoria equation (Articles index is at end). LAN allows creation of Serelles Secondary Line from Torrebotana Central Line [1,2]. Different relations have LAN role as common link: Riquelme de Gozy (RG) [2] [3] and [9], Flui Piep de Garberí (FPG) [4] and Silva de Peral y Alameda (SPA) [5,8]. Pepliz LAN empire is $LAN_{n\to\infty}$ or LAN(P65) vs. LAN(P050) in RG relation as has been introduced in first part of Pepliz LAN empire [10].

This article has following main axes:

1) Deepen $n_sp^x \to n_sp^{x-1}ns$ that occupies empire zone between P69 and P72 limits
2) LAN amplitude: concept, behaviour and implications
3) Ionization energy obtained by Gozy method (IE Gozy method)
4) Annex or expansion with other empire zones and representation based on P69

KEYWORDS

RG relation, Tete-Vic equation, LAN, Pepliz LAN empire, Pepliz LAN empire limits: external and internal, LAN(P50), LAN(P65), Gozy IE calculation.

INTRODUCTION

Peplin LAN empire map and limits are explained in [10]:

P68 Pepliz LAN empire limits
P69 Internal limit of Pepliz LAN empire in $n_sp^x \to n_sp^{x-1}ns$
P70 Internal limit of Pepliz LAN empire in $n_ss^x \to n_ss^{x-1}ns$
P71 Internal limit of Pepliz LAN empire in $n_sp^x \to n_sp^{x-1}np$ and $n_ss^2 \to n_snp$
P72 External limit of Pepliz LAN empire for $n_sp^x \to n_sp^{x-1}ns$.
P73 External limit of Pepliz LAN empire for $n_sp^x \to n_sp^{x-1}np$ and and $n_ss^2 \to n_snp$

First point is to delve into $n_sp^x \to n_sp^{x-1}ns$ that occupies empire zone between P69 and P72 limits. Likewise, general vision between n_s=[2,4] and with $3s^x \to 3s^{x-1}ns$ where also P70 and P71 limits intervene is given. Abbreviations Table is at end article.

1) LAN(P65) vs. LAN(P50) in $n_sp^x \to n_sp^{x-1}ns$

1.A) LAN(P65) vs. LAN(P50) in $2p^x \to 2p^{x-1}ns$

According P65, Linearity between $LAN_{n\to\infty}$ (also called LAN(P65)) and LAN(P050) in RG, $2p^x \to 2p^{x-1}ns$ is developed with all cases where first two destiny n are present ($2p^{x-1}3s$ and $2p^{x-1}4s$) in [12] so that LAN(P65) can be known by applying RG linearity [10].

Table 1 summarizes jumps studied with Term and J of excited states and non-excited state is indicated by its ionization energy (IE) [11]. Isoelectronic series are in **Figure 1**.

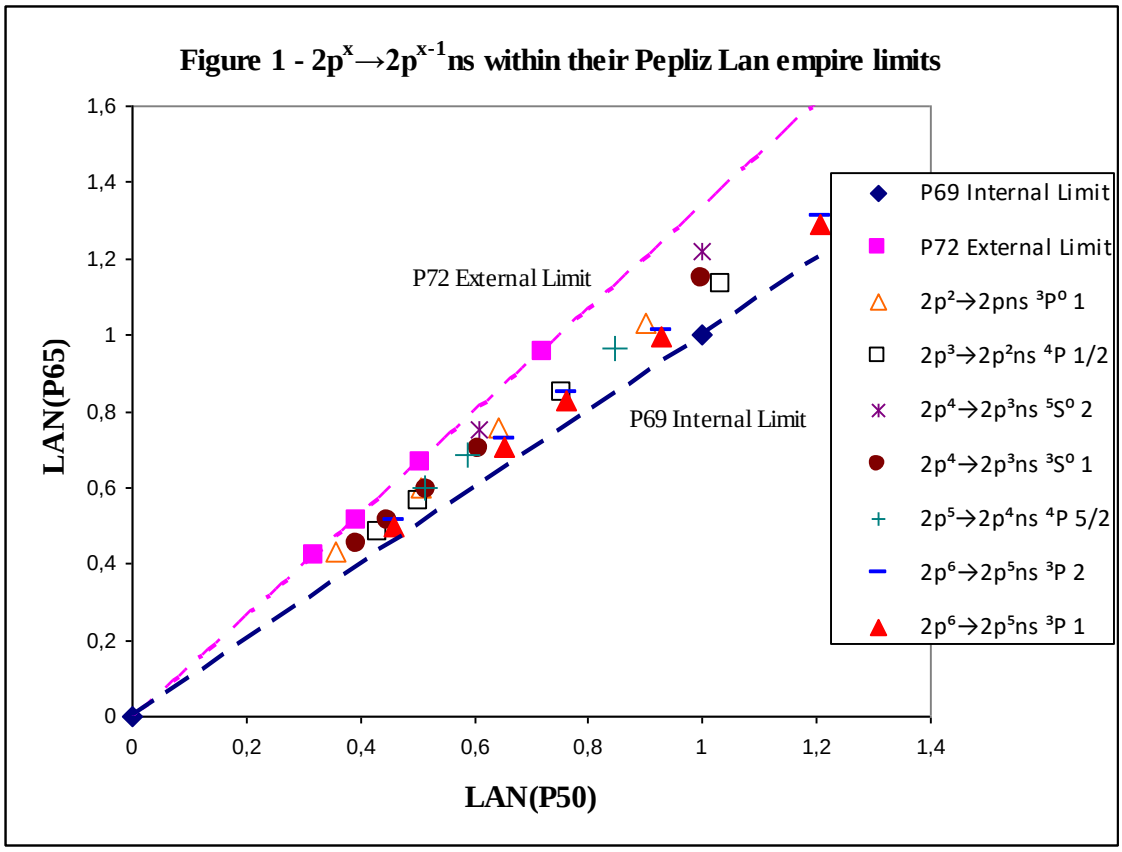

Table 1 - Isoelectronic series in $2p^x \rightarrow 2p^{x-1}ns$ represented in Figure 1.

Line	Series	Electron Jump	Term	J	Isoelectronic series
I	B	$2p \rightarrow ns$	^2S	1/2	[B I, O IV] [a]
II	C	$2p^2 \rightarrow 2pns$ [b]	$^3P^0$	1	C I, N II, O III and Ne V
III	N	$2p^3 \rightarrow 2p^2(^3P_0)ns$	^4P	1/2	N I, O II, Ne IV and Na V
IV	O	$2p^4 \rightarrow 2p^3(4S^0)ns$	$^5S^0$	2	O I y Ne III
V	O	$2p^4 \rightarrow 2p^3(4S^0)ns$	$^3S^0$	1	O I and [Ne III, Al VI]
VI	F	$2p^5 \rightarrow 2p^4(^3P_2)ns$	^4P	5/2	Ne II, Mg IV and Al V
VII	Ne	$2p^6 \rightarrow 2p^5ns$ [c]	^3P	2	[Ne I, Al IV]
VIII	Ne	$2p^6 \rightarrow 2p^5ns$ [d]	^3P	1	[Ne I, Al IV] and S VII

[a] $LAN_{n\rightarrow\infty}$ for O(IV) with small IE modification that allows RG linearity for first three jumps (2p→3s, 4s and 5s). IE reference is -77.4135 [11] and is changed to -77.2679. IE modification also affects LAN(P50). IE estimation method based on RG linearity is

developed later in present article. Electron jumps marked with [b], [c] and [d] have alternative configuration expression in [12]:
[b] $2s^2 2p(^2P^0_{1/2})ns_{1/2}$ Term=$(1/2,1/2)^0$ and J=1.
[c] $2p^5(^2P^o\ 3/2)ns$ Term=$^2[3/2]^0$ and J=2.
[d] $2p^5(^2P^o\ 3/2)ns$ Term=$^2[3/2]^0$ and J=1.

Relevant aspects in Figure 1:

A) All $2p^x \rightarrow 2p^{x-1}ns$ jumps are located between their limits: P69 Internal limit where LAN(P65)=LAN(P50) and P72 External limit whose border is 2p→ns.

B) P65, Linearity between $LAN_{n\rightarrow\infty}$ and LAN(P050) in RG, can be better adjusted with second-degree polynomial regression. This polynomial adjustment can be interesting for:

* start n low as shown in Figure 1: $n_s=2$
* small start charge ($z_s = 1$ or 2)

Linear regressions R^2 coefficient is always higher than 0.9990 for $2p^x \rightarrow 2p^{x-1}ns$ jumps (**Table 2**) and is closer to 1 when low z_s are ignored or data with z_s higher. These linear regressions R^2 coefficient are slightly improved with second-degree polynomial regression.

Table 2 - $2p^x \rightarrow 2p^{x-1}ns$ R^2 and equation coefficient for linear regression (y=a+bx) and second-degree polynomial regression ($y=a+bx+cx^2$) in $2p^x \rightarrow 2p^{x-1}ns$ for 8 lines defined in Table 1.

	Linear			Second-degree polynomial			
Line	R^2	b	a	R^2	c	b	a
I	1,0000	1,3431	-0,0125	1,0000	0,0121	1,3304	**-0,0094**
II	0,9996	1,1025	0,0417	1,0000	-0,1280	1,2655	**-0,0050**
III	0,9993	1,0815	**0,0199**	1,0000	-0,1774	1,3411	-0,0647
IV	------	1,2032	0,0178				
V	0,9998	1,1242	**0,0219**	0,9999	0,0527	1,0489	0,0456
VI	0,9999	1,0974	0,0375	1,0000	-0,1526	1,3076	**-0,0315**
VII	0,9996	1,0696	0,0259	0,9998	-0,0573	1,1656	**-0,0116**
VIII	0,9999	1,0536	0,0200	0,9999	-0,0190	1,0854	**0,0079**

3) Y-intercept tends to 0. Y-intercept closest to 0 between two regressions is marked with background painted gray and letter in bold. Eight regressions made with selection of regression closest to Y-intercept=0 are in **Figure 2** where regressions grouping at origin (0,0) is verified.

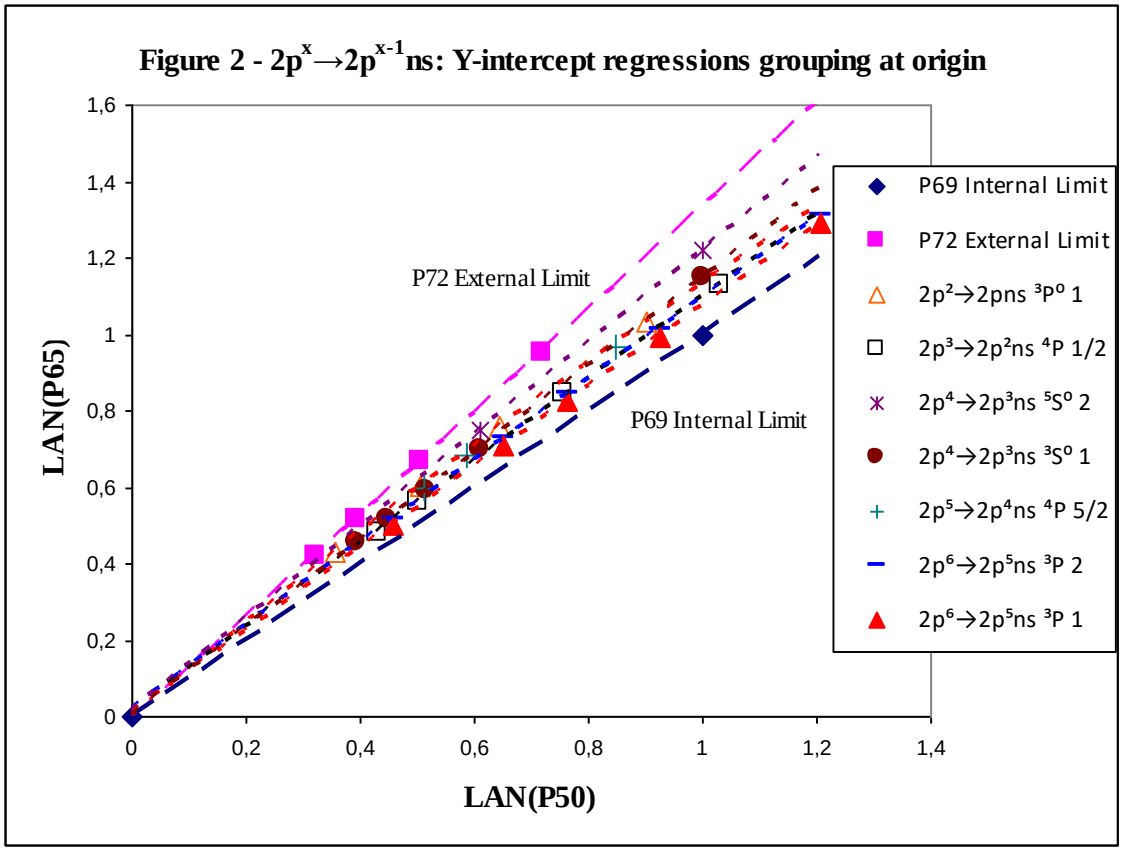

1.B) LAN(P65) vs. LAN(P50) in $n_sp^x \rightarrow n_sp^{x-1}ns$

Previous point is expanded to n_s equal to 3 and 4. Electron jumps are the same as those previously described and abbreviated from I to VIII in Table 1. **Table 3** contains isoelectronic series represented for n_s=3 (**Figure 3**) and n_s=4 (**Figure 4**). Coefficients of linear and second-degree polynomial regressions for $3p^x \rightarrow 3p^{x-1}ns$ are in **Table 4**.

Table 3 – Isoelectronic series for $3p^x \rightarrow 3p^{x-1}ns$ and $4p^x \rightarrow 4p^{x-1}ns$ in electron jumps indicates as Line (Table 1)

Line	$3p^x$ a $3p^{x-1}ns$	$4p^x$ a $4p^{x-1}ns$
I	Al I, Si II, S IV, K VII and Ti X	Ga I, Ge II, [Kr VI, Sr VIII] [c]
II	Si I and S III [a]	Ge I
III	P I, S II and Cl III [b]	Kr IV
IV	S I, Cl II and Ar III	Kr III, Rb IV and Sr V
V	S I, Cl II, Ar III and Sc VI	Kr III, Rb IV and Sr V
VI	Ar II	Kr II and Sr IV
VII	[Ar I, V VI]	[Kr I, Sr III] and Mo VII
VIII	[Ar I, Co X] except Mn VIII	[Kr I, Sr III] and Mo VII

[a] S III ionization energy is taken from [13] (-34.86 eV) instead of [11] (-34.79 eV). S III situation is between both Pepliz LAN empire limits, but Y-intercept→0 is more correct when [13] is used. There is little data to ensure that this change is correct.

[b] LAN(P65) of P I is calculated with jumps to 4s and 6s since 5s has not been found in [12].

[c] Kr VI, Rb VII and Sr VIII have only first jump (4p→5s) and next one (4p→6s) is simulated according to LAN_R amplitudes of isoelectronic series (in this case, Ga I and Ge II). LAN_R amplitude has only mentioned in [10] and is difference between two LAN_R. Broader explanation is developed in next point.

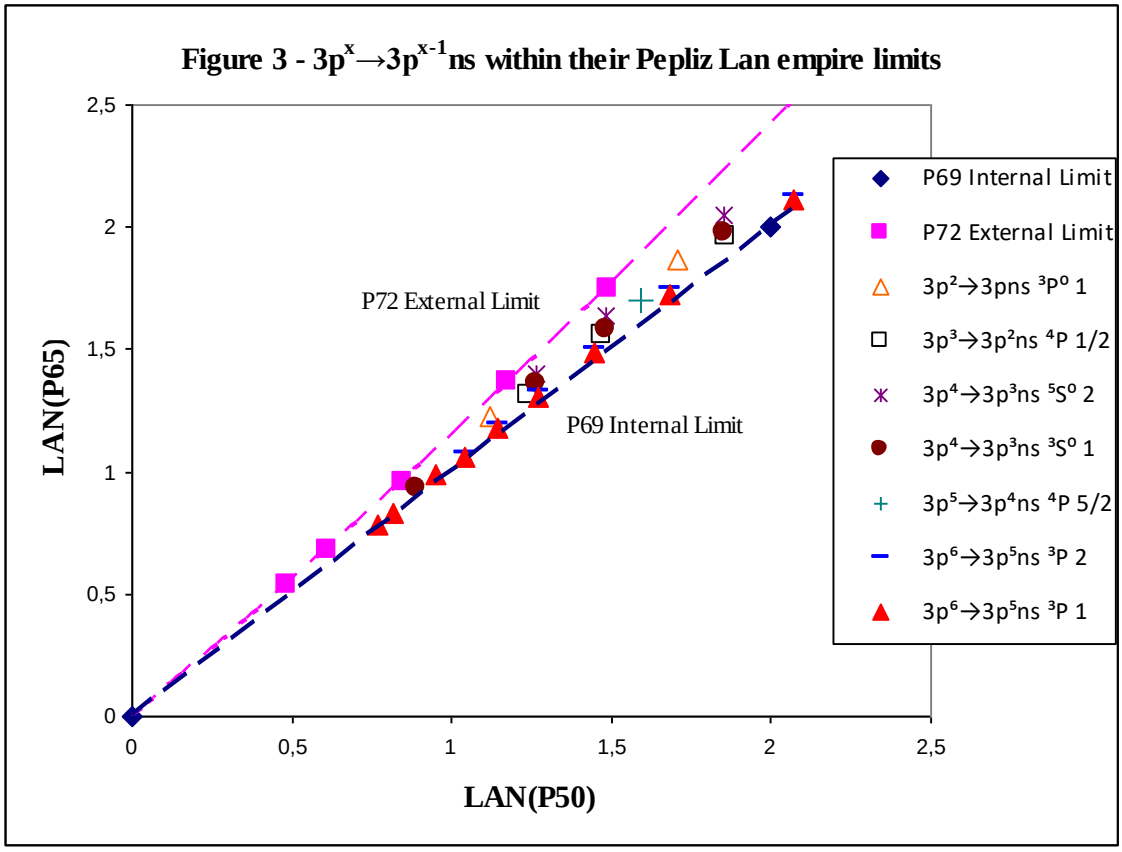

Table 4 - $3p^x \rightarrow 3p^{x-1}ns$ R^2 and equation coefficient for linear regression (y=a+bx) and second-degree polynomial regression ($y=a+bx+cx^2$) in $2p^x \rightarrow 2p^{x-1}ns$ for 8 lines defined in Table 1.

	Linear			Second-degree polynomial			
Line	R^2	b	a	R^2	c	b	a
I	1,0000	1,2097	-0,0576	0,9997	0,0649	1,0819	**-0,0038**
II	-----	1,0829	0,0154				
III	1,0000	1,0461	**0,0177**		-0,0331	1,1494	-0,0607
IV	1,0000	1,1011	**0,0056**		0,0161	1,0505	0,0443

V	0,9993	1,0767	**-0,013**	0,9993		1,0767	-0,013
VII	0,9998	1,0216	**0,0216**	0,9999	-0,0413	1,1500	-0,0726
VIII	0,9998	1,0196	**0,0071**	0,9999	-0,0256	1,0911	-0,0379

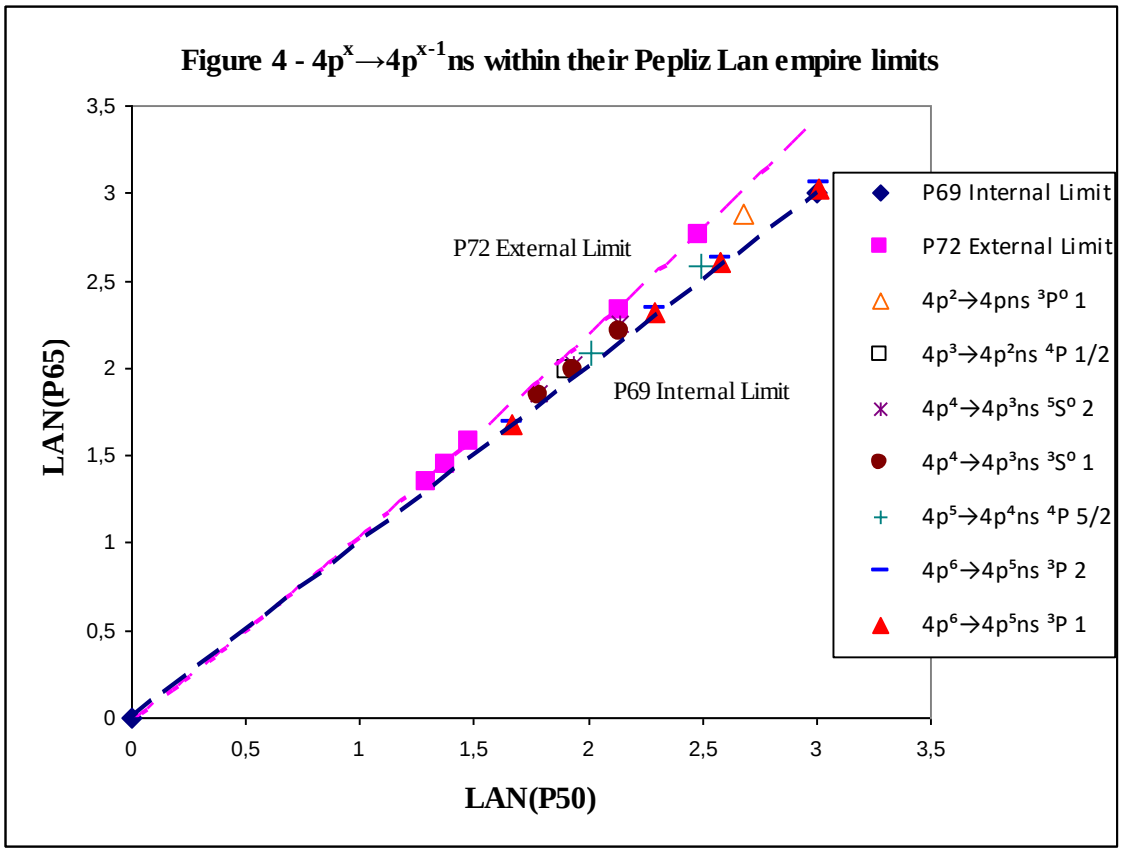

Is convenient to remember that, as Z increases, E_o is higher and therefore also curvature due to E_o relativistic excess (ER_o) [8] and [9]. Curvature can be noticeable affected even in first jumps (jumps with lower n). This error caused by curvature is magnified when LAN(P65) or $LAN_{n\to\infty}$ is calculated because is value extrapolated from this data in error by relativistic curvature. Study is stopped with $4p^x \to 4p^{x-1}ns$ (Figure 4) where E_o relativistic excess is already an important value ($ER_o \approx 600$ eV) for atom of highest Z treated (Molybdenum).

Figures 2, 3 and 4 are grouped in **Figure 5** to have Pepliz Lan map compliance global view for $n_sp^x \to n_sp^{x-1}ns$. Additionally, $3s^2 \to 3sns$ with their two possibilities according to spins, parallel (Term=^{3}S and J=1) or anti-parallel (Term=^{1}S y J=0), together with $3s \to ns$ (Term=^{2}S and J=1/2) join $n_sp^x \to n_sp^{x-1}ns$ in Figure 5. These 3 electron jumps, $3s^x \to 3s^{x-1}ns$ are explained in [10]. Three jumps direction is towards P70 internal limit and two zones are jumps location:

Between P69 and P70: $3s^2 \to 3sns$ (Term=^{3}S and J=1) and $3s \to ns$ (Term=^{2}S and J=1/2).
Between P70 and P71: $3s^2 \to 3sns$ (Term=^{1}S y J=0).

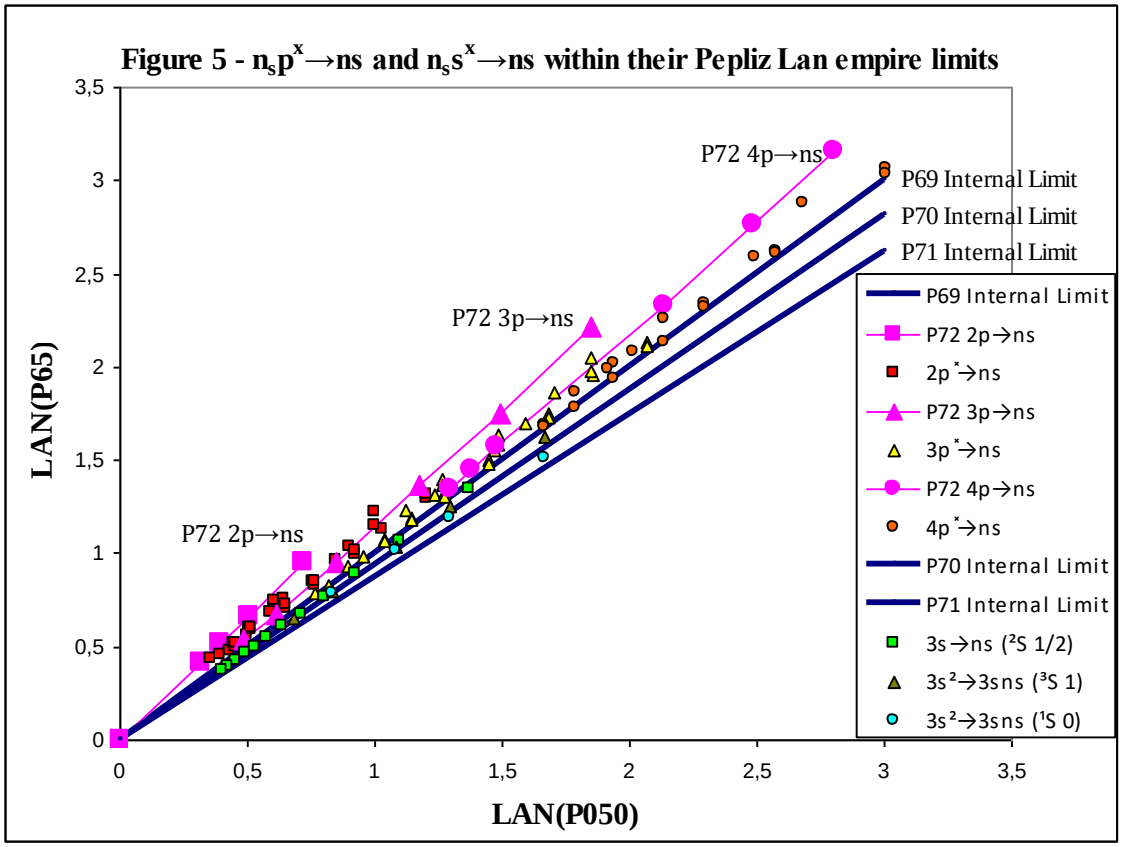

2) LAN amplitude: JLA vs. LAN(P50).

Jump LAN_R amplitude (JLA) is defined in (1) and Global LAN_R amplitude (GLA) in (2). JLA is amplitude between two consecutive n and GLA is difference between LAN_{START} or LAN_S and LAN(P65) or $LAN_{n\rightarrow\infty}$

$$(1)\ JLA = LAN_{R,\ n=x} - LAN_{R,\ n=x+1}$$

$$(2)\ GLA = LAN_S - LAN(P65)$$

Established order in (1) and (2) is made so that generally result is positive

Study LAN_R amplitude behaviour allows to use it with two objectives in this introduction:

A) Be extremely sensible tool for understand relativist excess.

B) Simple initial method to intuit variations in LAN_R. Some anomalies in RG relation that may cause doubts about reference data and require modifications are:

* Possibly IE consequence: Variation in global trend of linearity and curvature by relativistic effects with respect other closer isoelectronics (with similar z_s) of same jump.

* Possibly E_k consequence: Alternating discontinuities or single one discontinuity within RG relation. This point is developed in annex.

LAN_R amplitude behavior introduction

Figure 6 shows JLA vs. LAN(P50) for 2s→3s electron jump in Lithium isoelectronic series. According to (1), JLA(2s→3s)=LAN(2s)-LAN(3s)=LAN(P50)-LAN(3s). First two Li isoelectronic series members together with origin point (0,0) provide JLA base curvature through second degree polynomial regression. Subsequent Li series members move away from JLA base curvature as z_s increases. Return movement towards JLA base curvature must be done considering relativistic excess: ER_o and ER_{dR}. Be extremely sensible tool can be tested with small E_k or E_o variations in LAN calculation that imply significant alterations in situation of points represented.

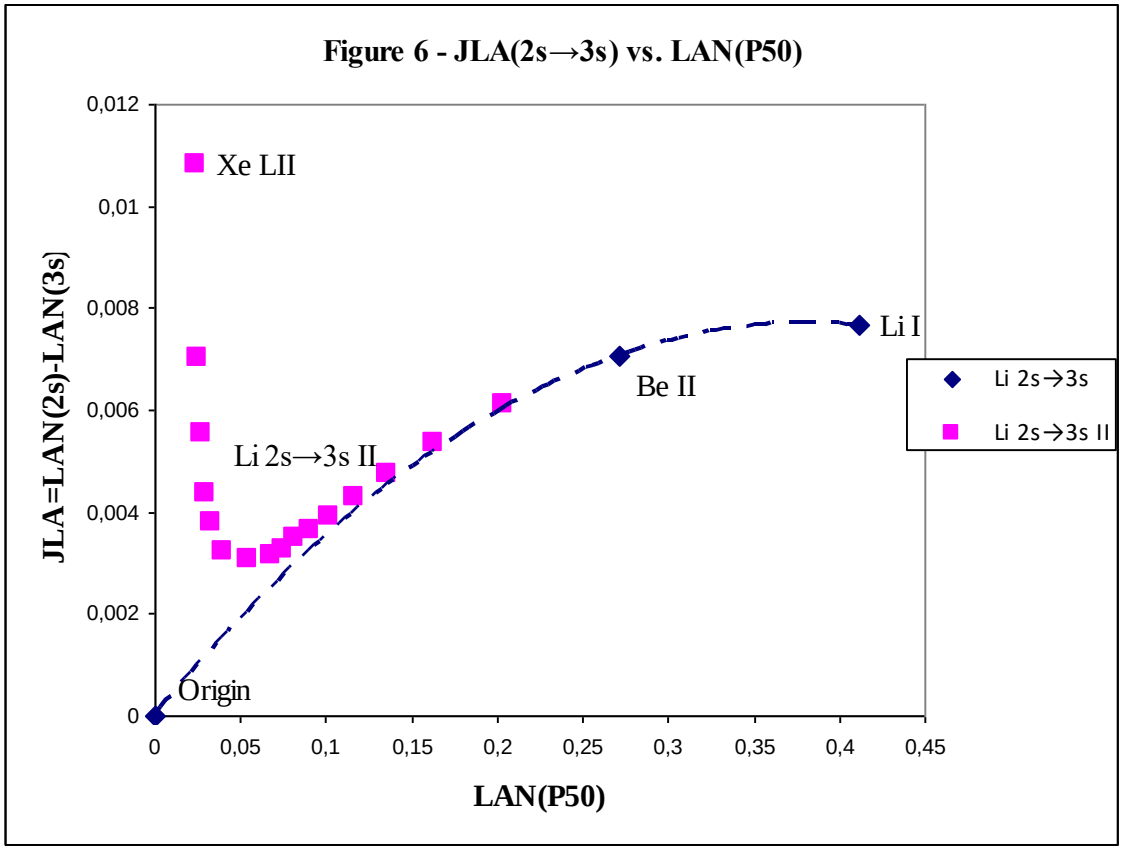

Figure 7 incorporates Na isoelectronic series to Figure 6. Series members are detached from JLA base curvature as z_s increases. P74, Pepliz LAN law: JLA vs. LAN(P50) behaviour, is now inscribed because is more understandable after this introduction and with help of Figure 6 and 7.

P74 Pepliz LAN law: JLA vs. LAN(P50) behavior.

JLA vs. LAN(P50) presents JLA base curvature adjustable with second degree polynomial regression with ending in origin point (0,0) and in which all isoelectronic series members are integrated.

* Isoelectronic series members are detached from JLA base curvature as z_s increases if relativistic effects are not considered.
* Behaviour of different isoelectronic series with same jump type form global whole. This global whole implies comparable JLA vs. LAN(P50) curves or, as in $n_s s \rightarrow ns$, maximums line that crosses maximums from origin point (**Figure 7**)

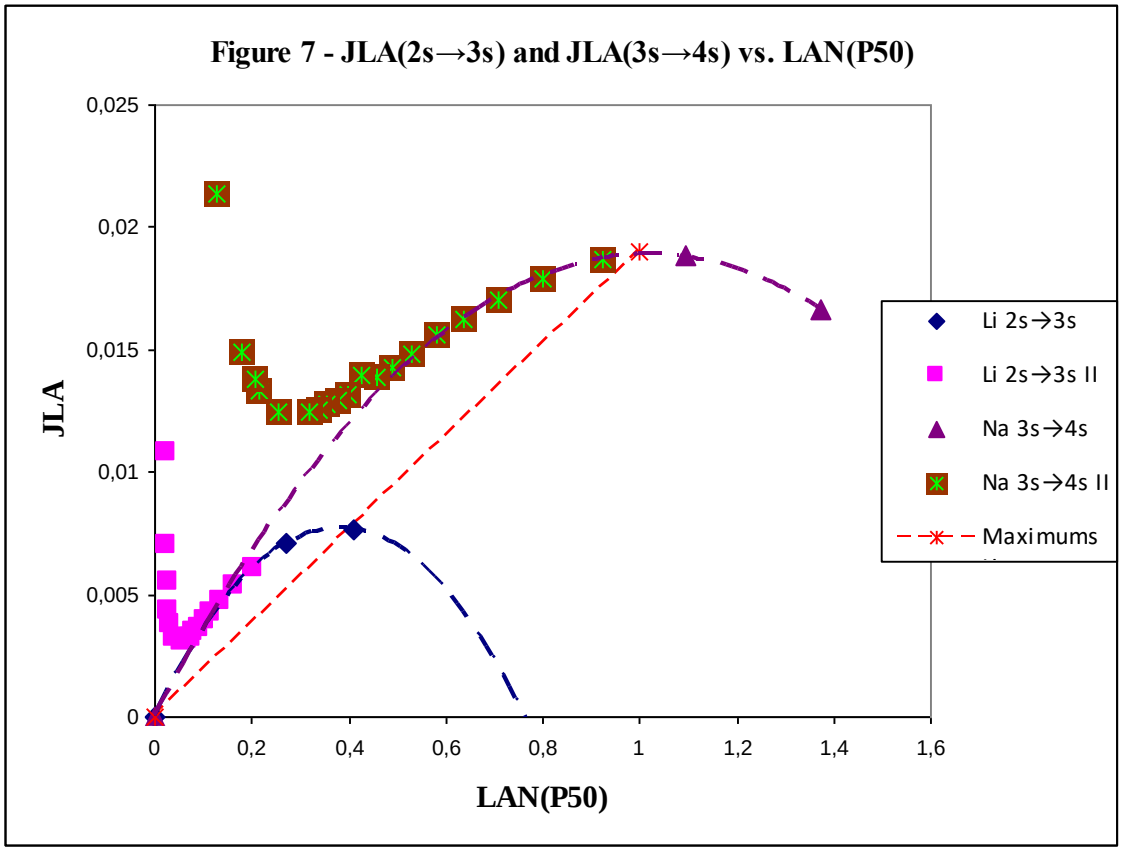

Figure 8 also adds following two start n: n_s=4 and 5:

* Maximums line is still line that crosses maximums from origin point.
* Position of intermediate z_s manifests directed movement as isoelectronic series n_s increases:
  - n_s=2 From beginning are located above JLA base curvature (Figure 6)
  - n_s=3 Situation on JLA base curvature (Figure 7)
  - n_s>3 Location below JLA base curvature (Figure 8)

SPA relation studies behaviour in isoelectronic series (atomicity behaviour) as P74 Pepliz LAN law: JLA vs. LAN(P50) behaviour. For this reason, comparison is interesting with Relativistic excess example in SPA relation [8] where also behaviour change when n_s increasing is observed. As happen in [8] example, comparison when n_s increases must consider change in relativistic excess balance between ER_o and ER_{dR}.
* In any case, isoelectronic series members location is above JLA base curvature when z_s is high.

* Cu isoelectronic series members from Ga III are attached Rb isoelectronic series instead of being next to K isoelectronic series.
* Cu isoelectronic series members with high z_s are above JLA base curvature as mentioned before. These member are Xe XXVI, Cs XXVII and Ba XXVIII and are indicated as "Xe, Cs, Ba" in Figure 8. Total E_o relativistic excess for Xe is calculated with (3) [8,10].

$$(3)\ 1s\ ER\ (Xe) = E_{oT} - E_o = -13.6056899*54^2\ eV + 41299.71\ eV = -39674,19175 + 41299.71\ eV = 1625.52\ eV$$

Xe XXVI happens to be on JLA base curvature of Rb isoelectronic series if there is E_o relativistic excess loss around 239 eV in 4s→5s, i.e. $ER_o \approx 239\ eV \rightarrow E_{om} = -41299.71\ eV + 239.71\ eV = -41060\ eV$. This fact is feasible if is considered that (3) is quite superior and shape of P64 Feliz representation of E_o vision from electron as moves away [8]. Anyway, this calculation is only first approximation since ER_{dr} has not been considered despite having considerable energy values:

$IE(Xe\ XXVII) = -857.03\ eV$ [11] for $LAN_R(4s)$

$E_{dR}(4s \rightarrow 5s) = -499.48\ eV$ [12] for $LAN_R(5s)$

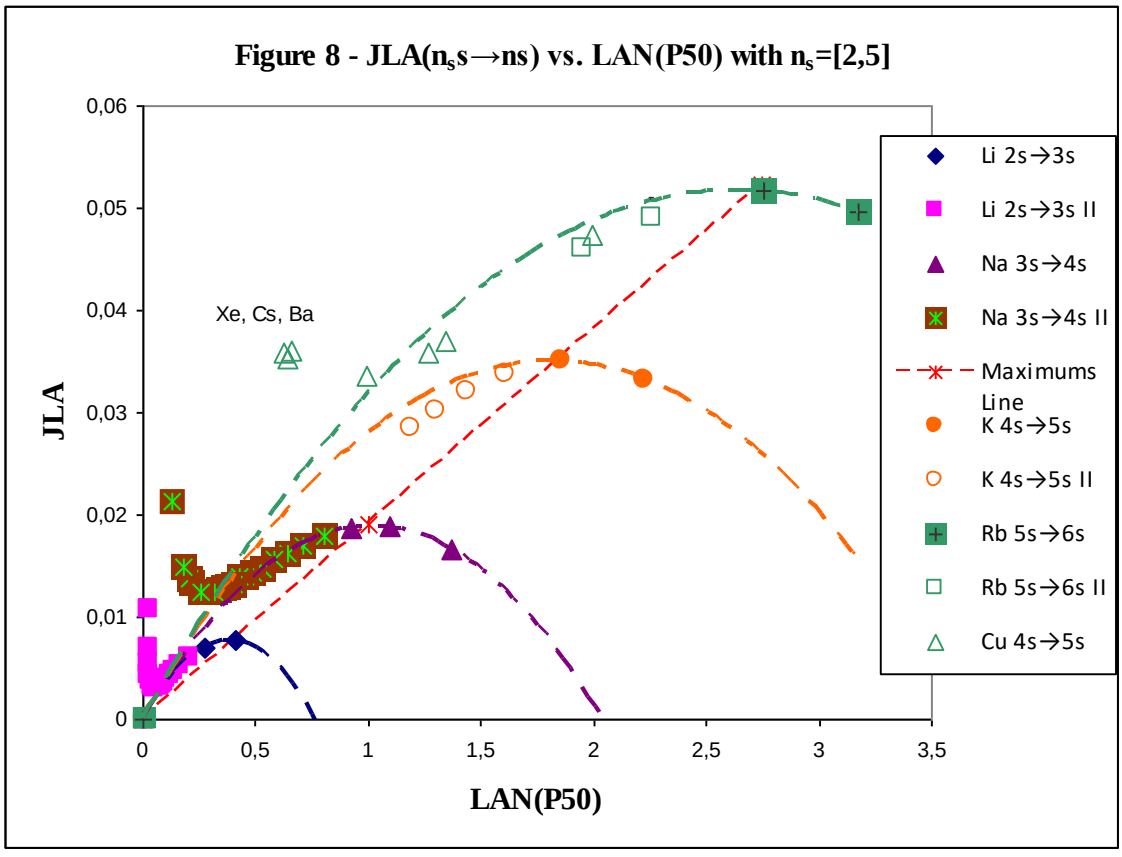

Other electron jumps following JLA ($n_ss \rightarrow ns$) vs. LAN(P50) guideline

Other electron jumps following JLA ($n_ss \rightarrow ns$) vs. LAN(P50) guideline are commented briefly.

Figure 9 adds two possibilities for $2p^6 \rightarrow 2p^5ns$ integrated in Table 1 as Line VII and VIII:

VII Term=^{3}P and J=2 or $2p^5(^2P^o\ 3/2)ns$ Term=$^2[3/2]^0$ and J=2. As "2" in Figure 9
VIII Term=^{3}P and J=1 or $2p^5(^2P^o\ 3/2)ns$ Term=$^2[3/2]^0$ and J=1. As "1" in Figure 9

Figure 9 maintains grade 2 polynomial regressions of $n_ss \rightarrow ns$ to compare locations and behaviours in P74 Pepliz LAN law: JLA vs. LAN(P50) behaviour. Result is satisfactory: there is good analogy between $n_ss \rightarrow ns$ and $n_sp^6 \rightarrow n_sp^5ns$ and $n_sp^6 \rightarrow n_sp^5ns$ tends to be located in direction marked by $n_ss \rightarrow ns$ polynomial regressions. **Figure 10** realizes same comparison and with similar positive results between $n_ss \rightarrow np$ and $n_ss \rightarrow ns$. Some concrete electron jumps have different behaviour. For example, $n_ss^2 \rightarrow n_snsnp$ has notable differences (**Figure 11**):

* Does not present parable curve seen in Figures from 6 to 10. In fact, points are practically adjusted with linear regression.
* Sorting is reverse. Therefore, lower start n implies being located with higher /JLA/ for same LAN(P50).
* $n_ss^2 \rightarrow n_snsnp$ has JLA positive and negative:
  Term=$^3P^0$ and J=1 JLA>0
  Term=$^1P^0$ and J=1 JLA<0

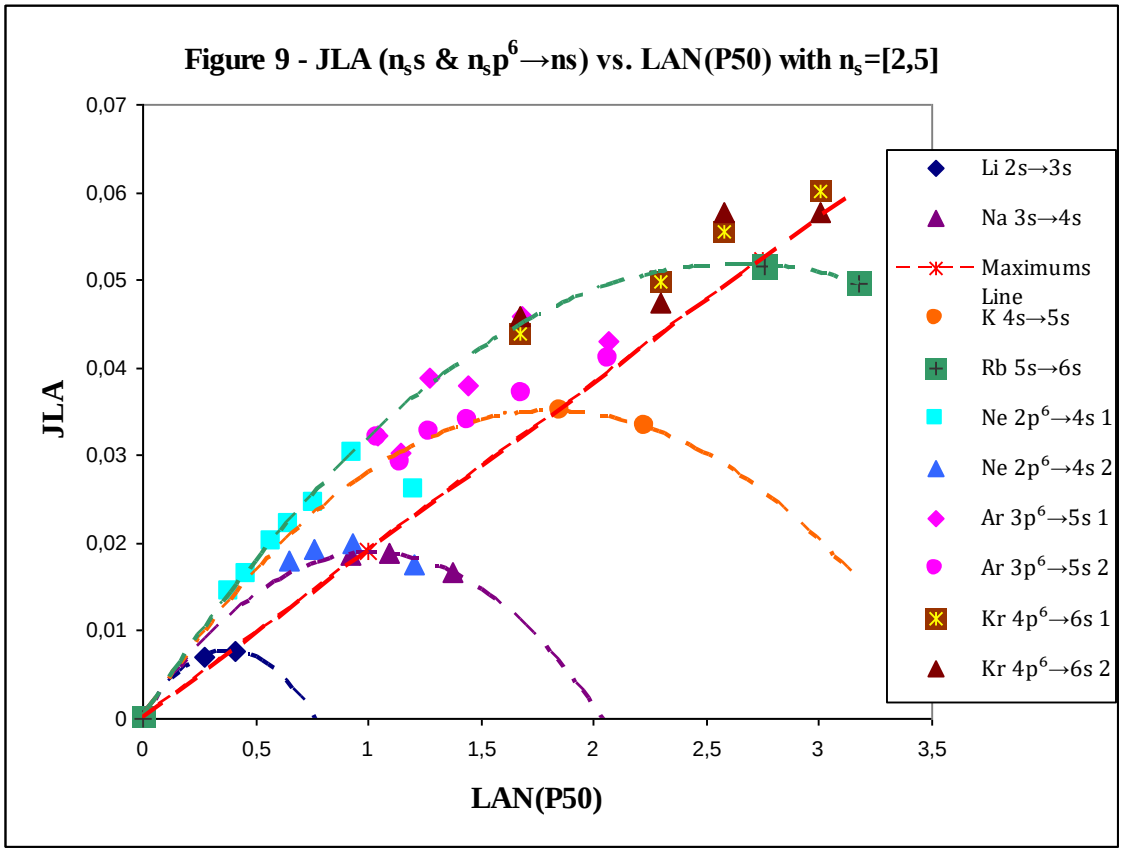

Figure 10 - JLA($n_s s \rightarrow ns$ & np) vs. LAN(P50) with n_s=[2,5]

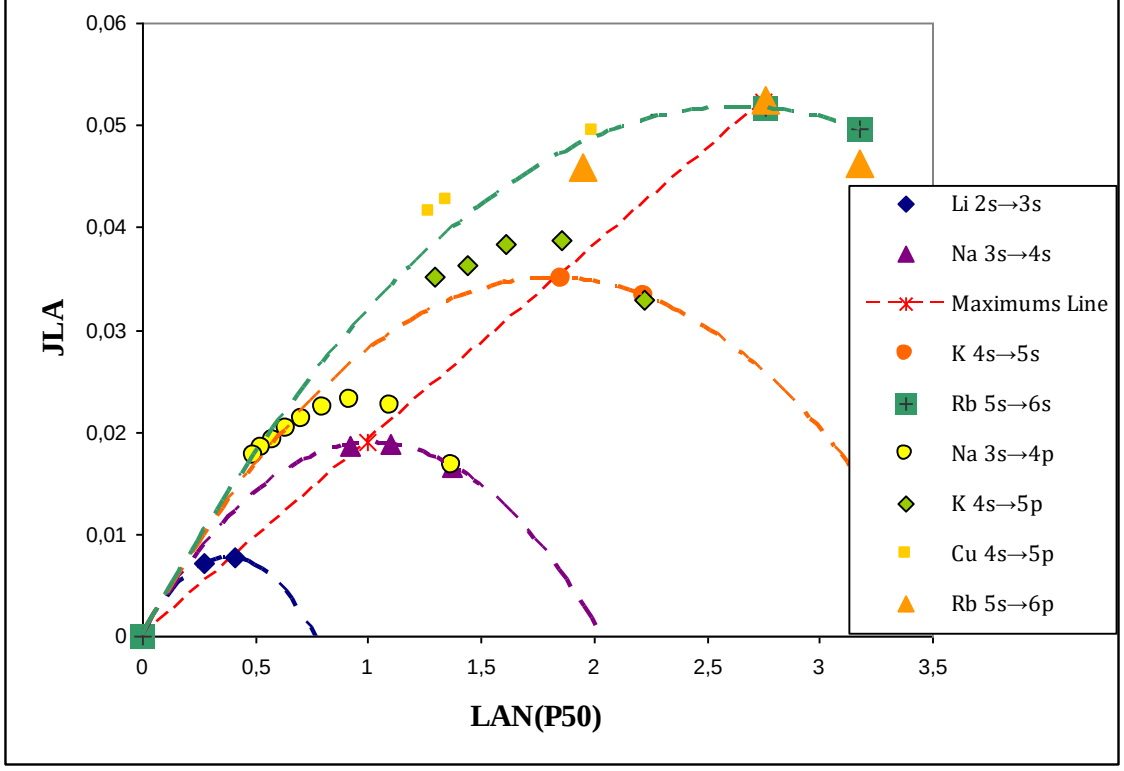

Figure 11 - JLA($n_s s^2 \rightarrow n_s np$) vs. LAN(P50) with n_s=[2,5]

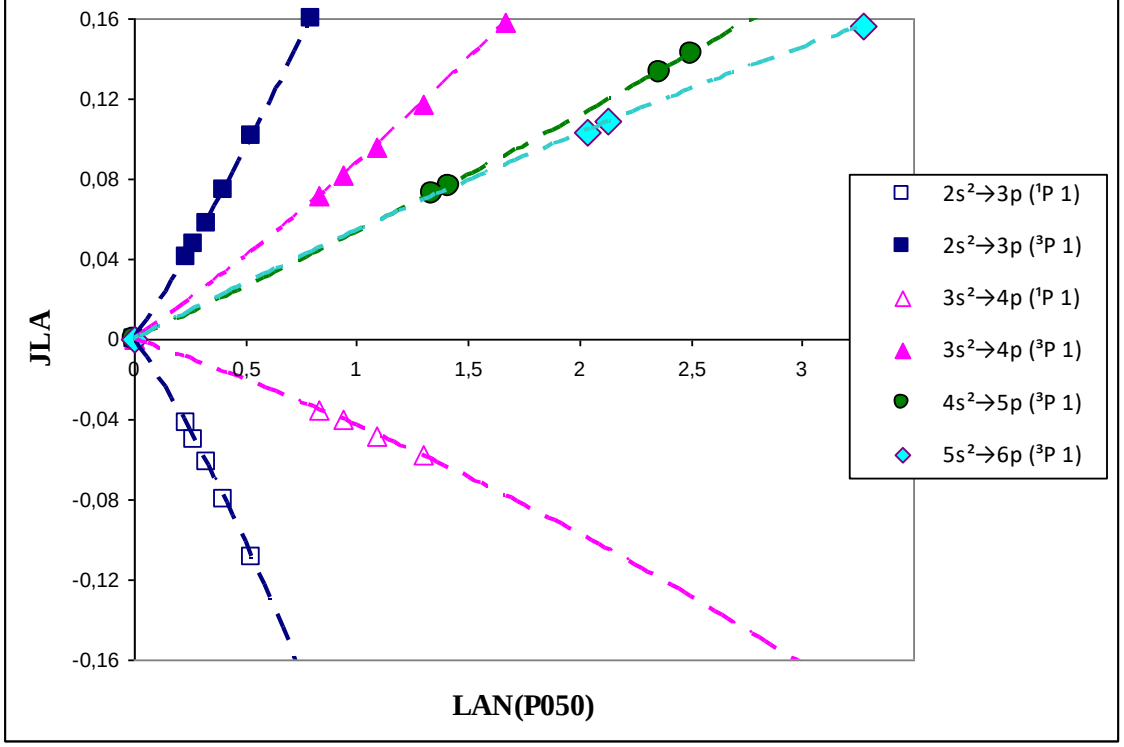

3) Ionization energy obtained by Gozy method (IE Gozy method)

Three energies that meet RG (Relation of Riquelme de Gozy) linearity are needed to discover IE (ionization energy): energies of three excited states or, in special $n_s s \rightarrow ns$ situation, only two excited states because its initial state also complies RG relation (P50). Excited states selected are those with lowest start n (n_s) since relativistic drift due to 1s ionization energy (E_o) is increased with n.

According to equation started in [1] and [2] for reference LAN or LAN_R (1):

$$(1)\text{ - LAN} \approx -LAN_R = \left(\frac{z_s^2 E_o}{z_o^2 E_{dR}}\right)^{1/2} - n = \left(\frac{z_s^2 E_o}{z_o^2 (E_k + IE)}\right)^{1/2} - n$$

Equations (2), (3) and (4), where n is principal quantum number of least excited state, are obtained when (1) is applied for energies contributed (E_{k1} E_{k2} and E_{k3}) to reach excited states and whose associated LAN are LAN_{R1}, LAN_{R2} and LAN_{R3}.

$$(2) - LAN_{R1} = \left(\frac{z_s^2 E_o}{z_o^2 (E_{k1} + IE)}\right)^{1/2} - n = a + bE_{k1}$$

$$(3) - LAN_{R2} = \left(\frac{z_s^2 E_o}{z_o^2 (E_{k2} + IE)}\right)^{1/2} - n + 1 = a + bE_{k2}$$

$$(4) - LAN_{R3} = \left(\frac{z_s^2 E_o}{z_o^2 (E_{k3} + IE)}\right)^{1/2} - n + 2 = a + bE_{k3}$$

Three equations and 4 unknowns (LAN_{R1}, LAN_{R2} and LAN_{R3} and IE) are transformed into three equations and three unknowns (a, b and IE) thanks to RG relation. K_{LAN} (5) is included to abbreviate expressions.

$$(5) K_{LAN} = \frac{(-E_o)^{1/2} z_s}{z_o}$$

Next step is to obtain equations where Y-intercept (a) and slope (b) are in IE function. Slope (b) is in IE function (6) when is done: (3)-(2)

$$(6)\ b = \frac{\dfrac{K}{(-IE - E_{k2})^{1/2}} - \dfrac{K}{(-IE - E_{k1})^{1/2}} - 1}{E_{k2} - E_{k1}}$$

Y-intercept (7) is obtained from (3):

$$(7)\ a = \frac{K}{(-IE - E_{k2})^{1/2}} - n - 1 - bE_{k2}$$

(7) is transformed into (8) when b in IE function (6) is included:

$$(8)\ a = \frac{K}{(-IE - E_{k2})^{1/2}} - n - 1 - E_{k2}\frac{\frac{K}{(-IE - E_{k2})^{1/2}} - \frac{K}{(-IE - E_{k1})^{1/2}} - 1}{E_{k2} - E_{k1}}$$

Finally, expression (4) is equalized to zero (9) or (10). (11) is equation where a and b are included as IE function and consequently there is single unknown. n non-influence in IE calculation is demonstrated in (11).

$$(9)\ \frac{K}{(-IE - E_{k3})^{1/2}} - n - 2 - a - bE_{k3} = 0$$

$$(10)\ \frac{-K}{(-IE - E_{k3})^{1/2}} + n + 2 + a + bE_{k3} = 0$$

$$(11)\ \frac{-K}{(-IE - E_{k3})^{1/2}} + 1 + \frac{K}{(-IE - E_{k2})^{1/2}} - E_{k2}\frac{\frac{K}{(-IE - E_{k2})^{1/2}} - \frac{K}{(-IE - E_{k1})^{1/2}} - 1}{E_{k2} - E_{k1}} + E_{k3}\frac{\frac{K}{(-IE - E_{k2})^{1/2}} - \frac{K}{(-IE - E_{k1})^{1/2}} - 1}{E_{k2} - E_{k1}} = 0$$

IE Gozy method application

First example is IE Gozy method with outermost electron of ion Al IV: $2p^6 \rightarrow 2p^5(^2P\ 3/2)ns$ with Term and J pf $^2[3/2]$ and 2 or 3P y 2. Data are summarized in **Table 5** and belongs to [11] and [12] as happens with rest of data.

Table 5 - Al IV: $2p^6 \rightarrow 2p^5(^2P^o\ 3/2)ns$. Term and J $^2[3/2]$ and 2 or 3P y 2.					
K_{LAN} (5)			E_{ki} (eV)		
E_o (eV)	z_o	z_s	E_{k1} n=3	E_{k2} n=4	E_{k3} n=5
-2304,14	13	4	76,45414	99,42073	107,98923

IE Gozy method (11) gives result of IE_G=−119.99204 eV and references is -119.9924 eV implying very low (%) relative change between both ionization energies:

(%) Relative Change ≈ 0.0003%

IE_G is ionization energy with IE Gozy method.

Figure 12 is represented with 0.00001 eV differential in IE search. IE=−119.99204 eV is observed as closest point to zero en (11) deviation (Y-axis).

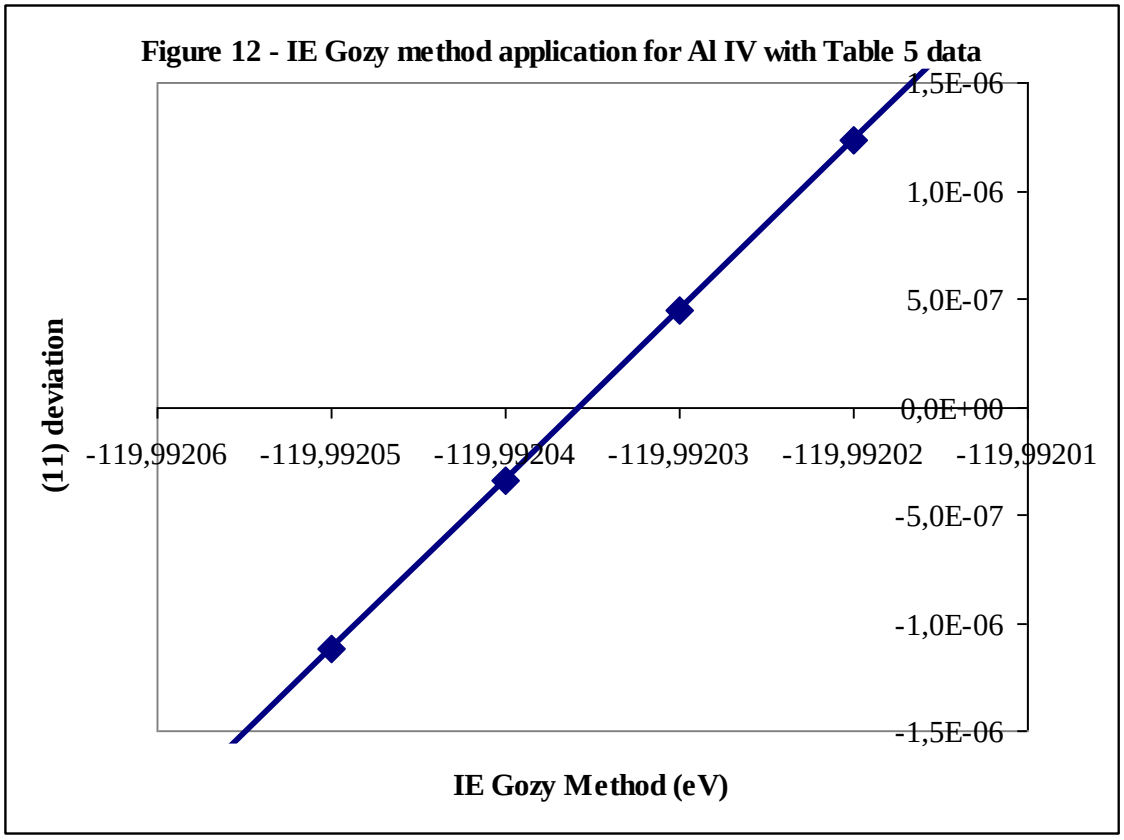

Four examples of Na and Li isoelectronic series have been compiled in **Table 6**. Electron jump selected for IE Gozy method is $n_s s \rightarrow ns$ with start n and first two excited states. Good approximation of IE Gozy method is confirmed by Table 6.

Table 6 - IE Gozy method for Li Na isoelectronic series with $3s \rightarrow ns$ (^2S 1/2). $E_{k1}=0$

Series	E (eV)	E_{k2}	E_{k3}	IE_G (ev)	IE [11]	IE_G-IE[11]	% RC
Na I	-1648,7021	3,1913531	4,1163588	-5,1394026	-5,1390767	-0,0003	-0,006 %
S IV	-3494,1892	45,00487	62,50073	-88,0629	-88,053	-0,0099	-0,011 %
Mn XV	-8571,9485	206,744	294,487	-435,5792	-435,172	-0,4072	-0,094 %
Fe XVI	-9277,6814	231,5702	330,05	-489,2202	-489,312	0,0918	+0,018 %
Li I	-122.454353	3,373129	4,340942	-5,391706	-5,39171476	8,761E-06	0,00016%
C IV	-489,993177	37,54849	49,76082	-64,49422	-64,49351	-0,00071	-0,00110%
S XIV	-3494,1892	399,242	535,575	-707,186	-707,01	-0,176	- 0,0249%
Ti XX	-6625,807	801,6806	1077,053	-1425,68	-1425,257	-0,423	- 0,0297%

LAN(P65) vs. LAN(P50) in $n_s p^x \rightarrow n_s p^{x-1} ns$ with IE Gozy method

Electron jumps with data in [12] but without IE [11] are selected to check compliance with P68 Pepliz LAN empire limits. IE is obtained from IE Gozy method (11) with first

three destiny n. This IE, called IE_G, is used for LAN(P65) and LAN(P50) calculation and represented in **Figure 13**. Points are located between their P72 and P69 limits as seen in Figure 3 where electron jumps have IE in reference [11].

Table 7 - IE Gozy method for isoelectronic members included in Figure 13			
Series	Excited State configuration	Member	IE_G (eV)
P	$3s^2 3p^2(^1D)ns\ ^2D\ 3/2$	S II	-24,7408
S	$3s^2 3p^3(^2D^0)ns\ ^1D^0\ 2$	S I	-12,1989
Cl	$3s^2 3p^4(^1D)ns\ ^2D\ 3/2$	Ar II	-29,3574
Ar	$3p^5(^2P^o\ 1/2)ns\ ^2[1/2]1$	Ar I	-15,9424
		K II	-31,8606
		Ca III	-51,2971
		Ti V	-99,8685
		Cr VII	-161,6789

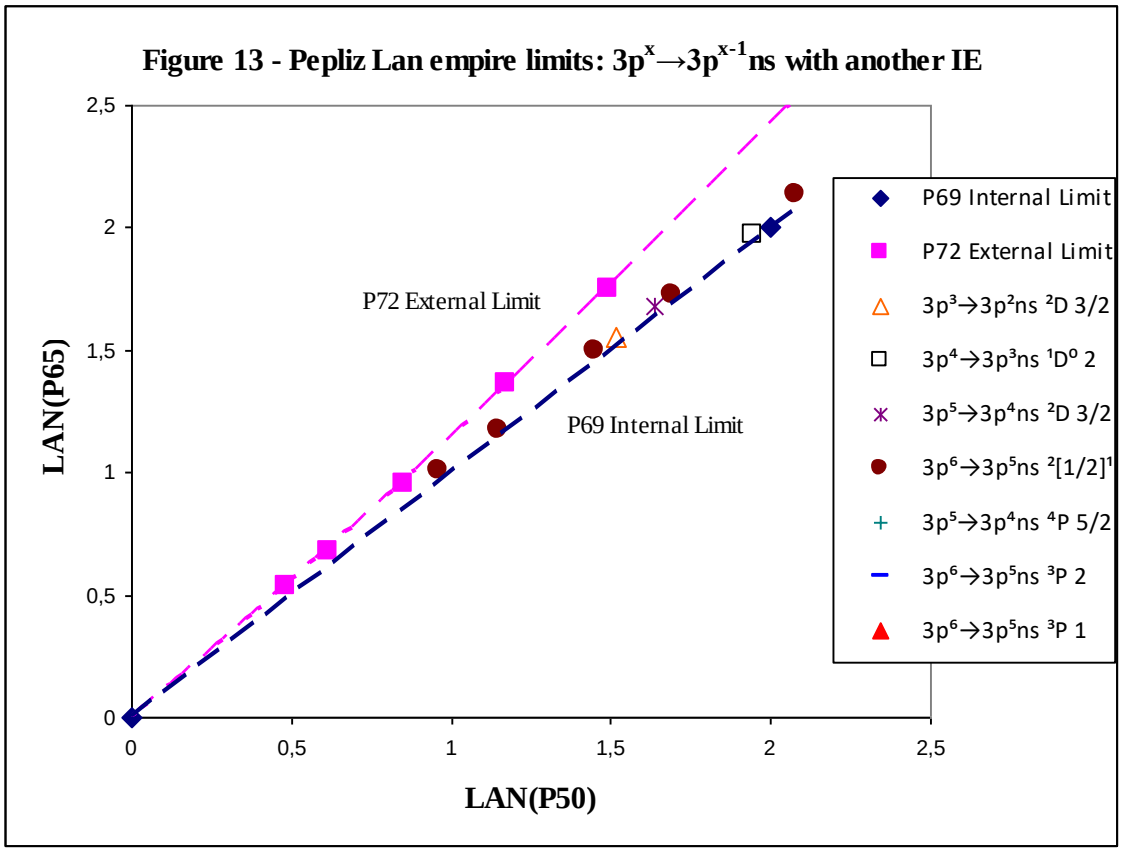

4) Annex or expansion with other empire zones and representation based on P69

4.1) $n_sp^x \rightarrow n_sp^{x-1}np$ and $n_ss^2 \rightarrow n_snp$ between P71 and P73 empire limits

Table 8 summarizes electron jump and associated isoelectronic series for **Figure 14**: $2p^x$ and $2s^2 \rightarrow np$ within their Pepliz Lan empire limits. Column Line indicates legend marked in Figure 14.

Three internal limits have been represented:

* P71 Be and P71 Mg are internal limits created by second degree polynomial regression of corresponding isoelectronic series.

* P71 uses formula: $\mathrm{LAN(P65)} = \frac{14+1/2}{16}\mathrm{LAN(P50)}$ [10]

Three internal limits are located in same border zone and another electron jumps do not cross these limits. **Table 9** uses identical electron jumps summarized in Table 8 for start $n = n_s = [3,5]$

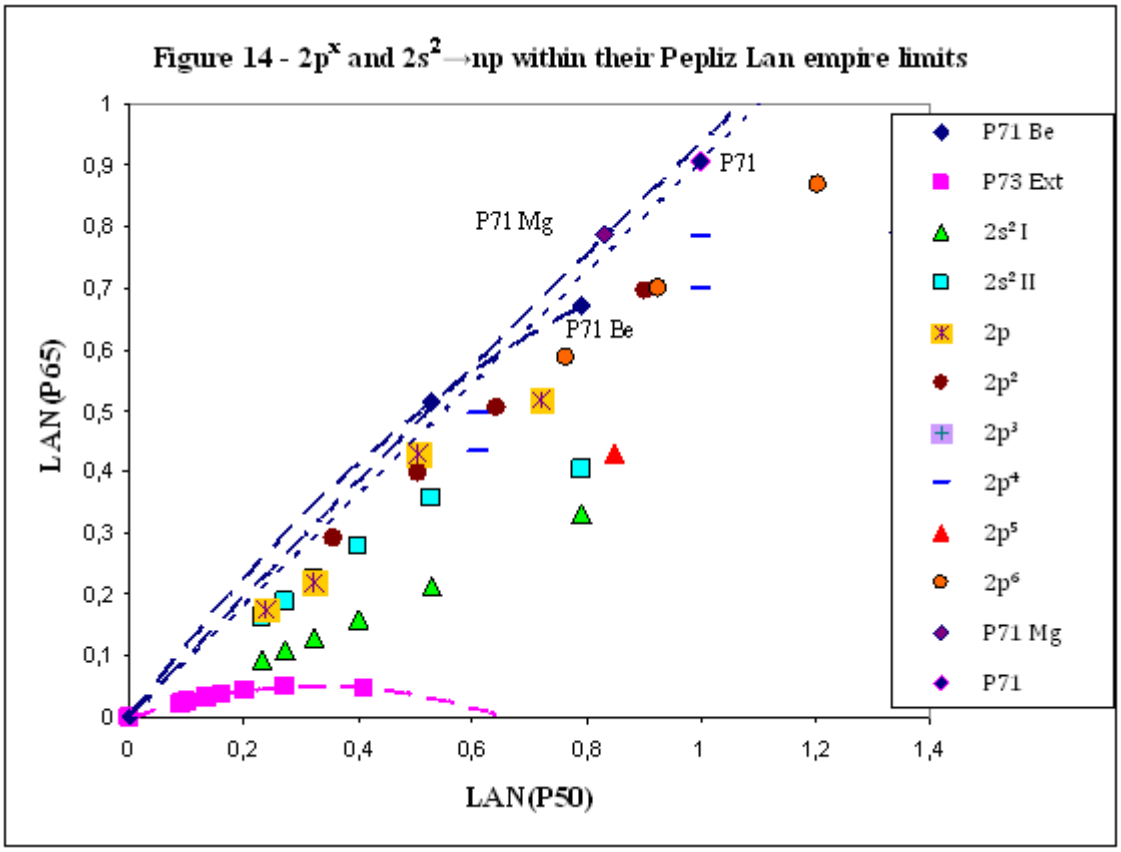

Table 8 - Isoelectronic series in $2p^x \rightarrow 2p^{x-1}np$ and $2s^2 \rightarrow 2snp$ represented in Figure 14.					
Line	Series	Electron Jump	Term	J	Isoelectronic series
P71 Be	Be	$2s^2 \rightarrow 2sns$	^1S	0	Be I and B II
P71 Mg	Mg	$3s^2 \rightarrow 3sns$	^1S	0	Mg I, Al II, Si III, S V and Ar

					VII
P73 Ext	Li	$2s \rightarrow np$	^2P	3/2	[Li I, Ne VIII]
$2s^2$ I	Be	$3s^2 \rightarrow 3snp$	$3P^o$	1	[Be I, O V] and Ne VII
$2s^2$ II	Be	$3s^2 \rightarrow 3snp$	$1P^o$	1	[Be I, O V] and Ne VII
2p	B	$2p \rightarrow np$	^2P	3/2	B I, C II, O IV and Ne VI
$2p^2$	C	$2p^2 \rightarrow 2pnp$	^1P	1	C I, N II, O III and Ne V
$2p^3$	N	$2p^3 \rightarrow 2p^2(3P)np$	$4D^o$	3/2	
$2p^4$	O	$2p^4 \rightarrow 2p^3(^4S^0)np$	^5P	1	O I and Ne III
$2p^4$	O	$2p^4 \rightarrow 2p^3(^4S^0)np$	^3P	2	O I and Ne III
$2p^5$	F	$2p^5 \rightarrow 2p^4(^3P)np$	$^4P^0$	5/2	Ne II
$2p^6$	Ne	$(^2P^0\ 3/2)np\ ^2[1/2]1$ (or $2p^5\ 3p\ \ 3S\ 1$)			Ne I, Na II and Mg III
Note: P71 uses formula: $LAN(P65) = \frac{14+1/2}{16} LAN(P50)$ [10]					

Table 9 - Isoelectronic series in $n_sp^x \rightarrow n_sp^{x-1}np$ and $n_ss^2 \rightarrow n_ssnp$ with n_s=[3,5] and represented in Figure 15, 16 and 17.

Line	Isoelectronic series		
	n_s=3	n_s=4	n_s=5
P71 __	P71 Mg: Mg I, Al II, Si III, S V & Ar VII	P71 Ca Ga: Ca I. Ga II (1)	
P73 Ext	[Na I, K IX]	P73 Ext K: [K I, Cr VI] P73 Ext Cu: Cu I, Ga III & [Kr VIII, Sr X]	P73 Ext Ru: Ru I, Sr II, Zr IV & Mo VI P73 Ag: Ag I & [Cs VIII, Ba X]
n_ss^2 I	[Mg I, S V]	Ca I. Ga II, Kr VII, Rb VIII & Sr IX (1)	In II, Xe VII, Cs VIII & Ba IX
n_ss^2 II	[Mg I, Co XVI] except Cl, Ca & Mn. Kr XXV	Ca I. Ga II (1)	In II, Xe VII, Cs VIII & Ba IX
n_sp	Al I & Si II	Ga I & Ge II	In I and Sn II
n_sp^2	Si I	Ge I & Kr V	Sn I (2)
n_sp^5	Ar II	Kr II & Sr IV	I I, Xe II & Cs III
n_sp^6	Ar I, Ca III & Sc IV	Kr I, Rb II & Sr III	Xe I, Cs II & Ba III
Note: P71 uses formula: $LAN(P65) = \frac{14+1/2}{16} LAN(P50)$ [10]			

(1) Ca I is not isoelectronics with rest of atoms.
(2) Sn I has been represented with IE obtained with IE Gozy method: -7,877842 eV.

Figure 15 - $3p^x$ and $3s^2 \rightarrow np$ within their Pepliz Lan empire limits

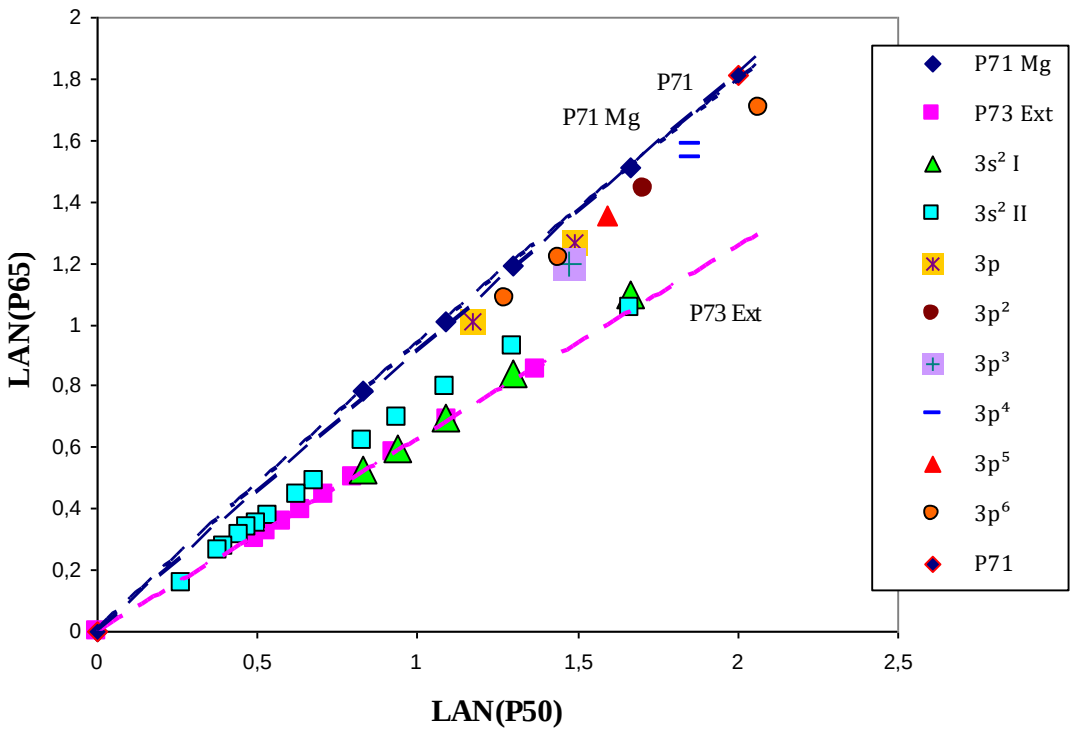

Figure 16 - $4p^x$ and $4s^2 \rightarrow np$ within their Pepliz Lan empire limits

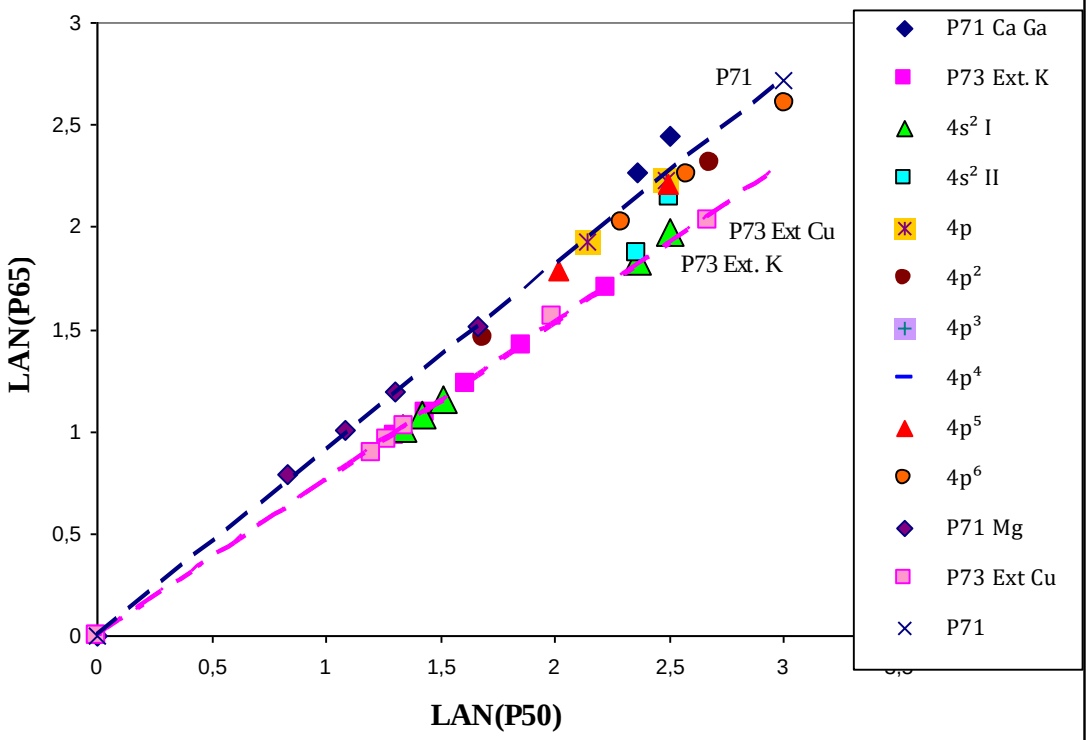

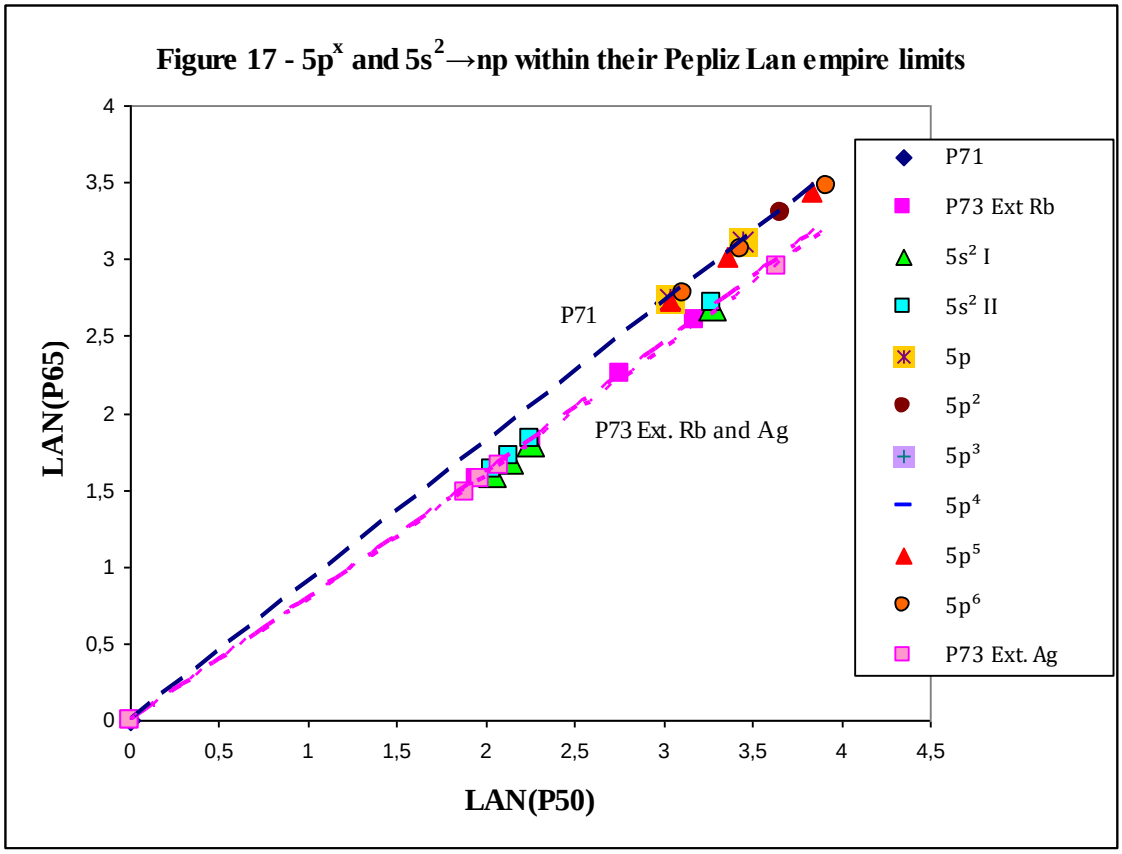

Following points are highlighted in view of figures from 14 to 17:

* Compliance with limits is carried out by different electron jumps.
* Different electron jumps seem to be attracted by Pepliz Lan empire limits as n_s increases. Electron jumps with n_s growth resemble that make movement leaving Pepliz Lan empire central zone and migrate towards border areas created in this case by P71 and P73.

Related to previous point, LAN increases with n_s and consequently region represented progressively occupies smaller figure space. For example in Figure 17, there are too many empty areas on either side of empire zone and quite less in Figure 15. Next representation is included to avoid this fact.

4.2) Representation referred to the Pepliz LAN empire limit

Representation referred to the Pepliz LAN empire limit consists of modifying Y axis when referenced with respect to one of empire limits. Simplest and fundamental representation is to do it with respect to P69 internal limit where LAN(P50)=LAN(P65). Way to do it is coordinates change: (x,y) → (x,y-x) that is:

Fundamental referenced representation: LAN(P65)-LAN(P50) vs. LAN(P50). Indicated briefly as: LAN(P65-P50) vs. LAN(P50) or as LAN(P65-P69) vs. LAN(P50) where reference limit origin is indicated.

Representation referred to the Pepliz LAN empire limit allows:

* Figure focused in empire zones: avoid empty areas
* Empty zones elimination allows better comparison between different n_s. General compliance of Pepliz LAN limits can be observed with Figure 5, but few more comparisons between different n_s.

Figure 18 with fundamental referenced representation comes from Figure 17 and is example of centred in empire zones.

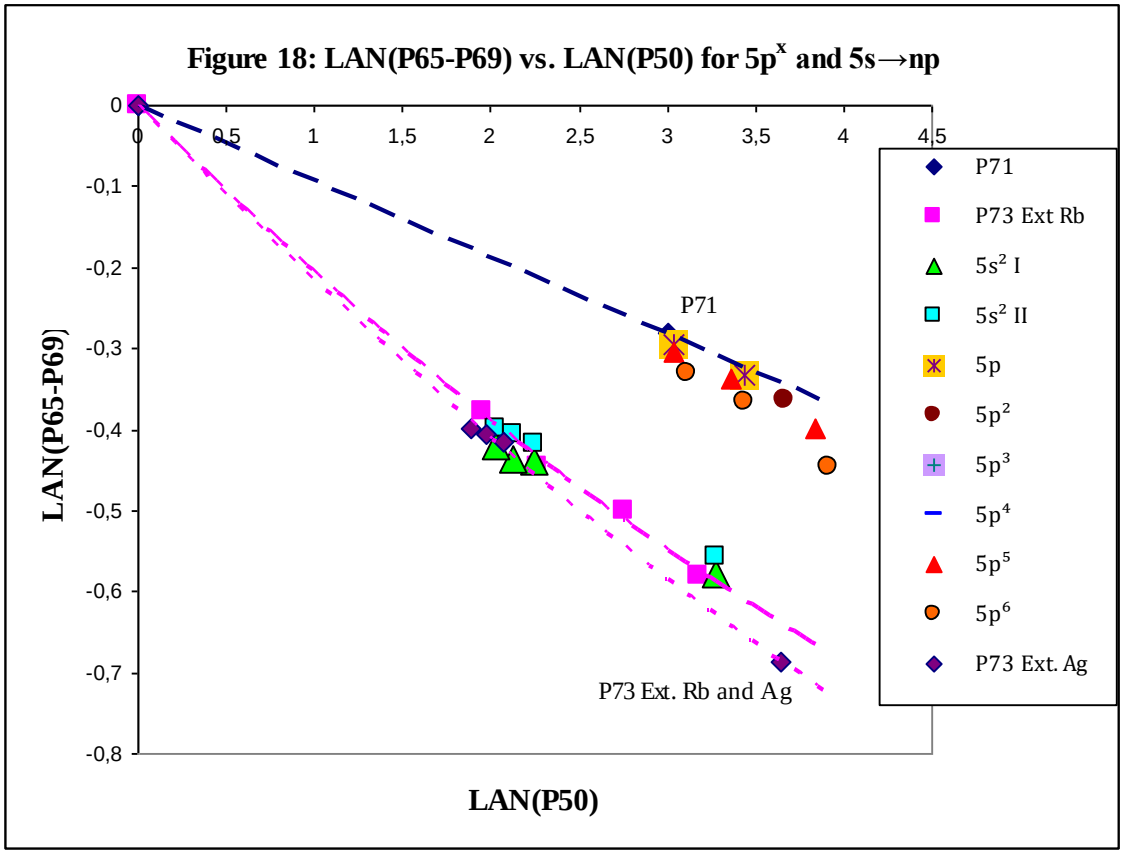

Figure 19 is like Figure 18 but referenced to $n_sp^x \rightarrow n_sp^{x-1}np$ and $n_s s^2 \rightarrow n_s snp$ internal limit: P71 internal limit. Therefore, Figure 19 is:

$$\text{LAN(P65)} - \frac{14+1/2}{16}\text{LAN(P50)} \text{ vs. LAN(P50)} \text{ . Indicated briefly as:}$$

$$\text{LAN}\left(\text{P65} - \frac{14+1/2}{16}\text{LANP50}\right) \text{ vs. LAN(P50)} \text{ or LAN(P65-P71) vs. LAN(P50)}$$

Figure 19 implies higher focus level in Pepliz LAN empire zone studied with respect to Figure 18. In turn, Figure 18 already has centring level superior to that seen in Figure 17. Trends and divergences are better observed with as focus level increases and this

focus allows divergences correction in more efficient way as is introduced in last and next point.

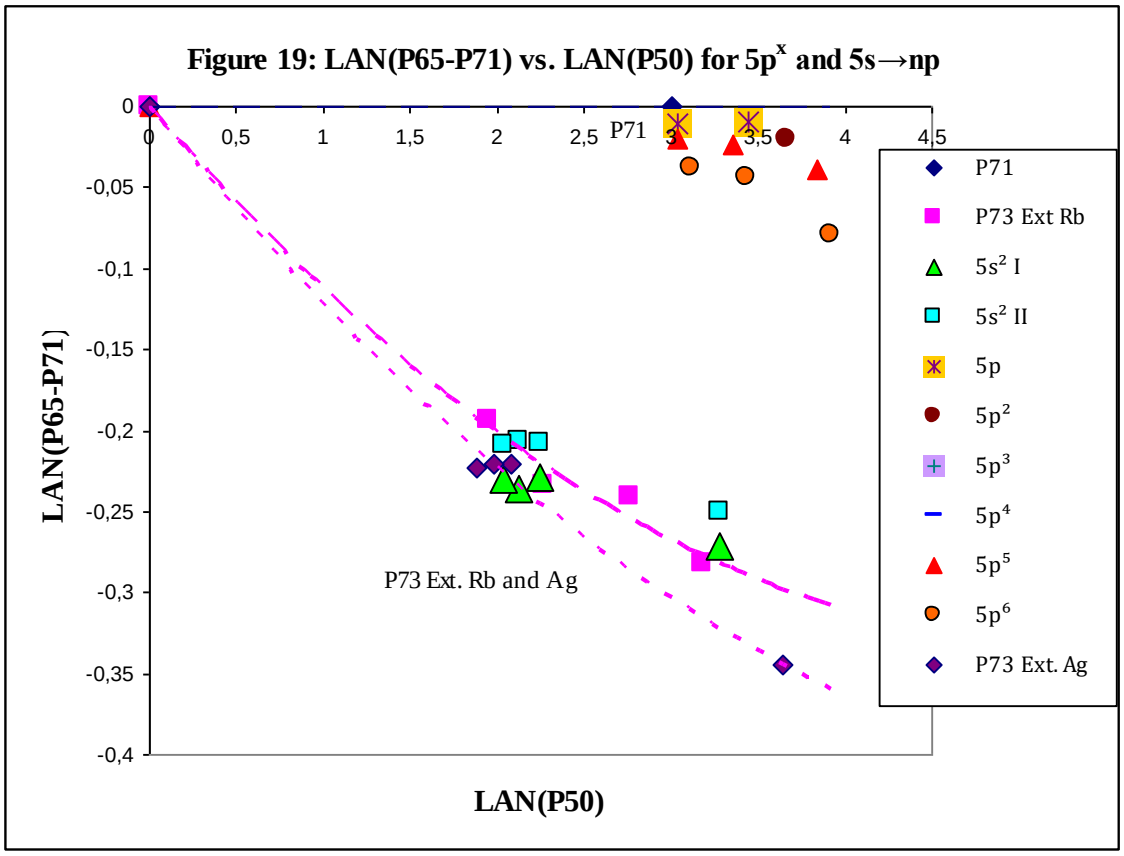

4.3) Divergence modification through JLA & LAN(P65-Limit) vs. LAN(P50)

Jump energy (E_k) divergence modification can be solved by several methods. High sensibility to small energetic variations and great concordance between reference values and estimates have been checked with three relations: Riquelme de Gozy (RG) and Silva de Peral y Alameda (SPA) for electron jump and Fly Piep de Garberi (FPG) for ionization energy [2,10]. Apparent deviations in SPA and RG have been corrected by excess relativistic introduction [8,9]. This point incorporates another information sourse to correct possible divergences by using:

* P74 Pepliz LAN law: JLA vs. LAN(P50) behavior.
* Representation referred to the Pepliz LAN empire limit or LAN(P65-Limit) vs. LAN(P50)

First example

Representation can be joint because X axis is identical in both cases (LAN(P50)): sign change or scale adjustment coefficient may be necessary. However, first example is made separately. Al I isoelectronic series with 3p→np (Term=$^2P^0$ and J=3/2) are selected. **Figure 20** is LAN(P65-P71) vs. LAN(P50) and **Figure 21** is JLA vs. LAN(P50). Figure 20 has P71 Internal limit of Pepliz LAN empire on X axis and P73

External limit of Pepliz LAN empire is provided by second degree polynomial regression of Na isoelectronic series with 3s→np electron jump. Points without asterisk are those corresponding to reference data and with asterisk have energetic modification. S IV is considered divergent point due to:

* Al I and Si II are closer to P71 internal limit and instead S IV moves away from internal and goes to P73 external limit.
* Al I and Si II has been represented in Figure 15 and meets seen with 2p→np (Figure 14), 4p→np (Figure 16) and 5p→np (Figure 17) and has been previously highlighted: electron jumps with n_s growth resemble that make movement leaving Pepliz Lan empire central zone and migrate towards border areas created in this case by P71 and P73. In this case, n_sp→np goes towards P71 internal limit. In addition, smaller distance of n_sp→np points to internal limit is observed in any of four figures.

Energetic modification considered is change in Ek(2) where 2 indicates second jump (3p→5p). **Table 10** shows $E_k(2)$ modification effects. LAN(P50) is not modified becacuse ionization energy (IE) has not been altered. $E_k(2)$ changes from 35.3722 [12] to 35.17 eV and implies Actual Change = AC = 0.2022 eV and Relative Change = RC = 0.57%. Effect is ≈350 and ≈600 times higher in RC % of LAN(P65-P73) and JLA respectively. This effect extension allows discontinuity to disappear successfully in both figures (Figure 20 and 21). Divergence can also have its origin in Ek(1) and or IE, therefore everything must be analyzed. Likewise, excess relativistic should be considered as reason for divergence.

Figure 20: LAN(P65-71) vs. LAN(P50) 3p→np Modifications

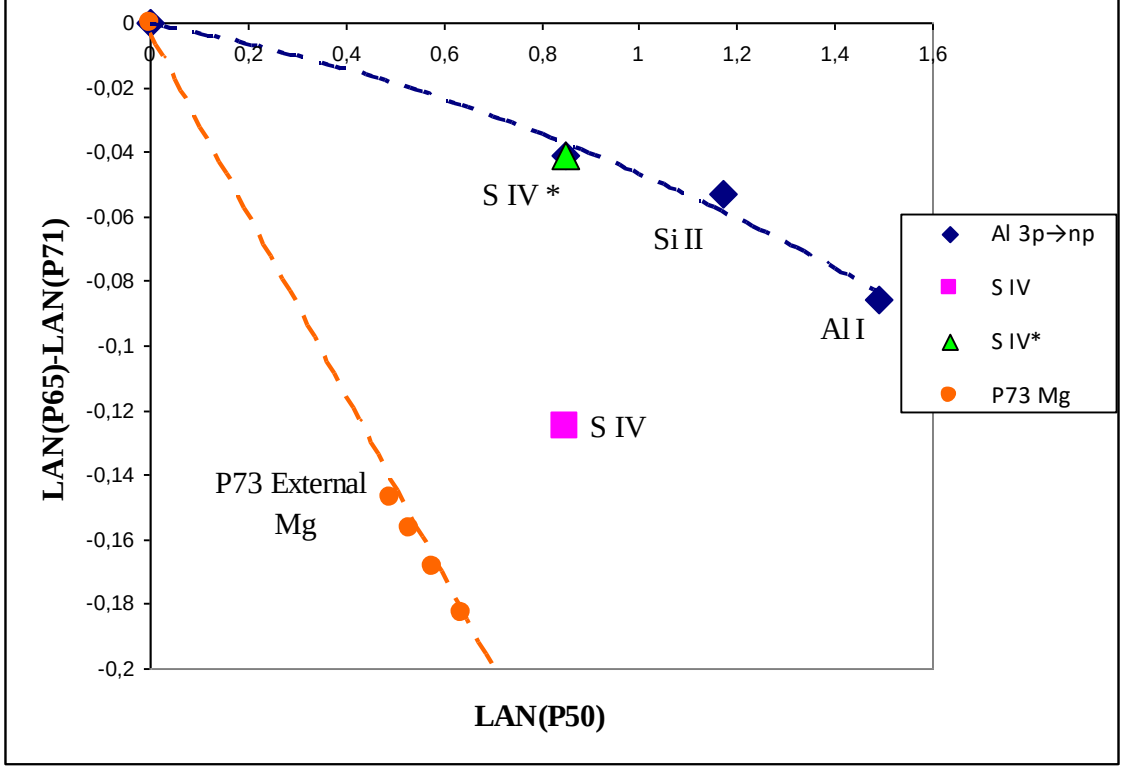

Table 10 $E_k(2)$ modification effects in 3p→np of Al isoelectronic series				
Series	LAN(P50)	LAN(P65-L)	JLA	$E_k(2)$
S IV	0,849492	-0,125205	0,0467160	35,3722
S IV*		-0,041321	0,0105515	35,17
AC	0 %	-0,08388381	0,03616453	0,2022
RC %		-203,00%	342,74%	0,57%

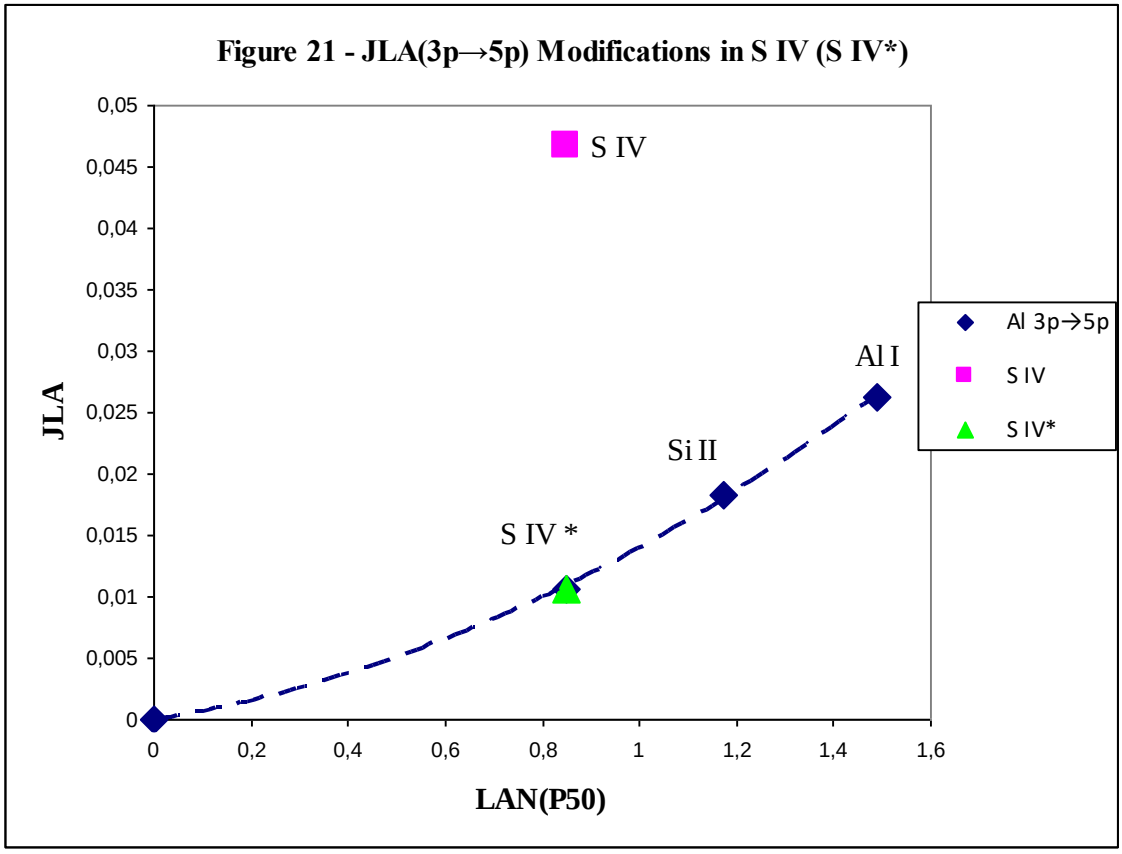

Second example

Al I isoelectronic series with $n_sp \rightarrow ns$ electron jump is second example. Al I and Si II are considered as correct and on their curves rest of isoelectronic series elements must be placed. Curves are JLA vs. LAN(P50) and LAN(P65-P69) vs. LAN(P50). Al I and Si II are considered as correct because:

* Very good linearity in relation of Riquelme de Gozy in Al I (destiny n=[4,11]) and Si II (destiny n=[4,9]) which are destiny n with reference data.
* JLA(3p→5s) overlap with JLA(4s→5s) vs. LAN(P50) of K isoelectronic series in 4s→5s (**Figure 22**).

S IV and K VII are only other two Al I series elements with data for second jump (3p→5s) [12] and both are clearly deviated from curve. Both points are represented as "Reference" in legend and as "S IV" and "K VII" in Figure 21. Modifications made on $E_k(2)$ allows to be installed on curve with "S IV*" and "K VII*" points. Deviations are taken in unison to correct LAN(P65-P69) vs. LAN(P50) curve (**Figure 23**) with same modifications in $E_k(2)$.

"M or C" indicated in Figures 21 and 22 is "Modificated or Created" and refers to points that have undergone modification (S IV and K VII changes to S IV* and K VII*) and also others that have been directly created because there is data for jump to 3p→4s, but there is no data for jump to 3p→5s [12]. $E_k(2)$ created is for Cl V and Ar VI and these created values manage to locate points Cl V* and Ar VI* in both curves at same time.

Table 11 $E_k(2)$ values: reference, modified and created for Al isoelectronic series in 3p→ns

Energy	Al I	Si II	S IV	Cl V	Ar VI	K VII
$E_k(1)$	3,1427211	8,121023	22,49671	31,7785	42,44	54,469
$E_k(2)$	4,6728907	12,146991	33,60231			81,0948
$E_k(2^*)$			33,54	47,4925	63,151	80,932

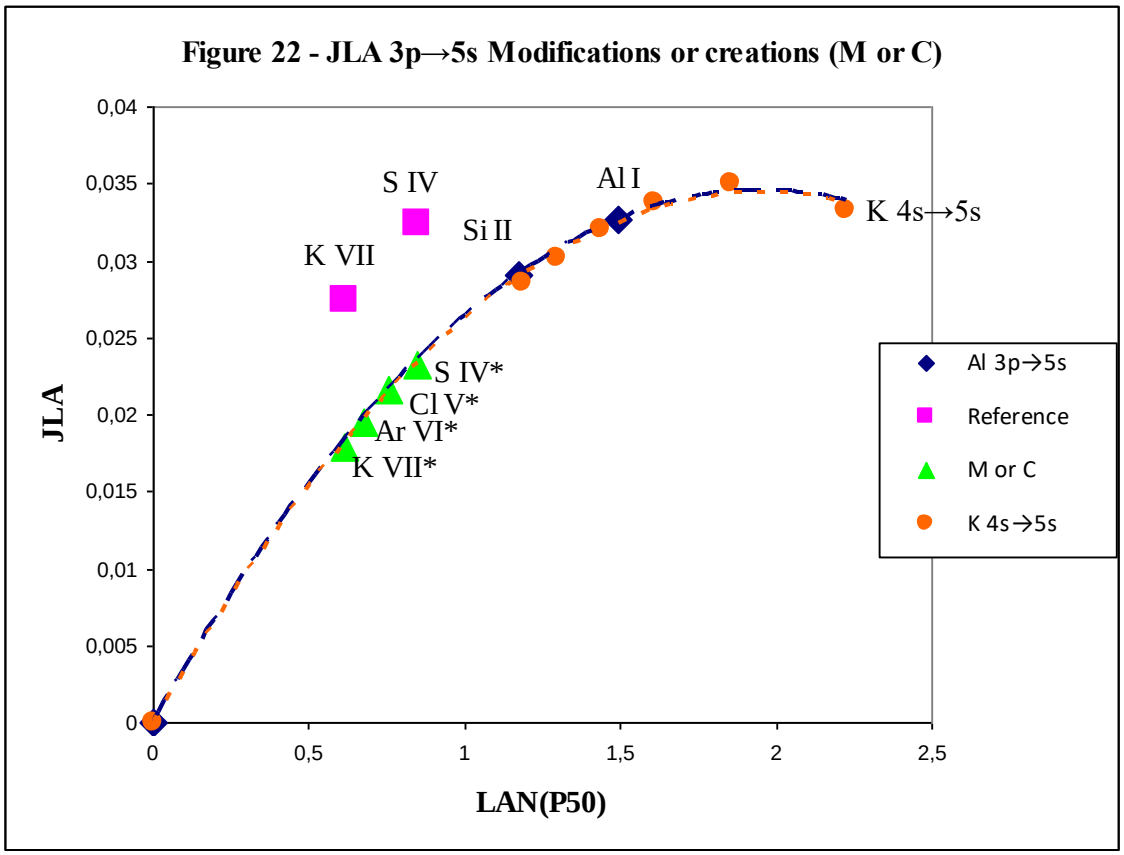

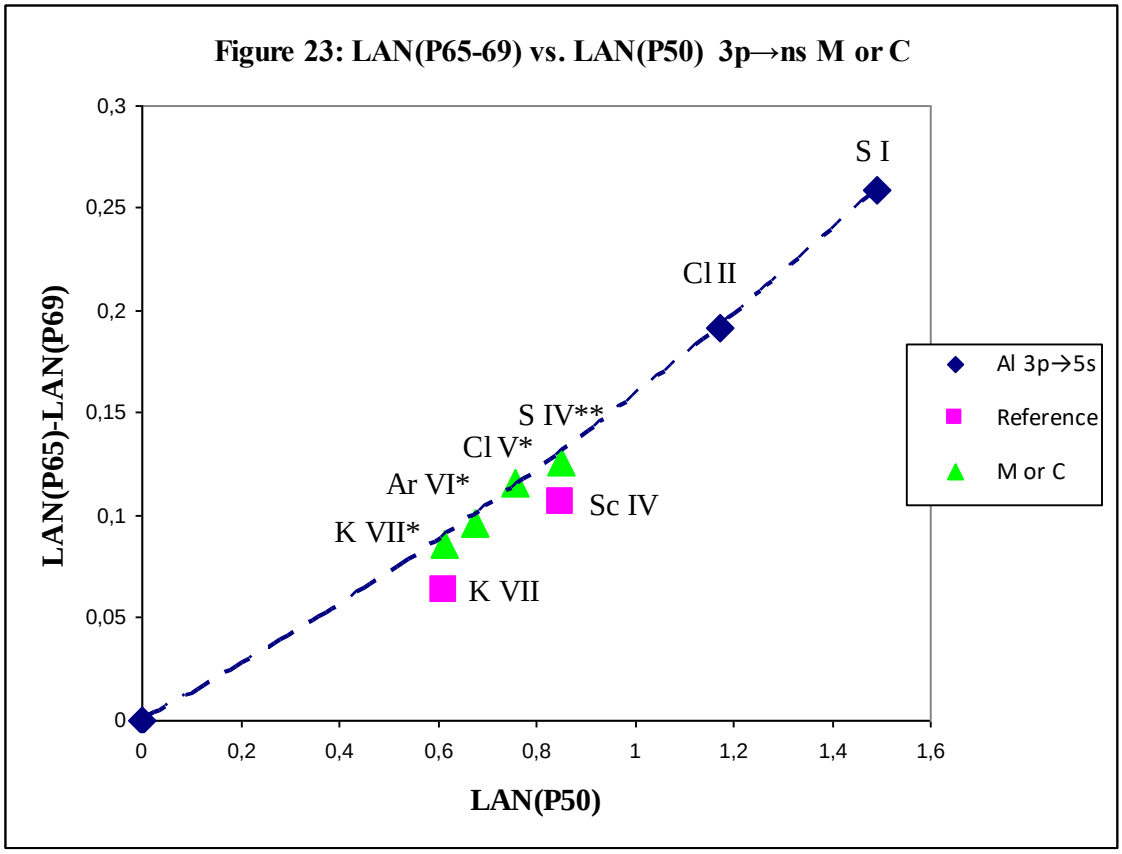

BIBLIOGRAPHY

[1] Javier Silvestre. Excited electrons by Torrebotana Central Line: Tete Vic Equation. Sent to: http://vixra.org/author/javier_silvestre

[2] Javier Silvestre. LAN plains for Tete Vic Equation. Sent to: http://vixra.org/author/javier_silvestre

[3] Javier Silvestre. Relation of Riquelme de Gozy: LAN lineality with energy of excited states. Sent to: http://vixra.org/author/javier_silvestre

[4] Javier Silvestre. Relation of Flui Piep de Garberí: LAN^{-1} and Ionization Energy. Sent to: http://vixra.org/author/javier_silvestre

[5] Javier Silvestre. Relation of Silva de Peral y Alameda: LAN interatomicity with energetic relation. Sent to: http://vixra.org/author/javier_silvestre

[6] Javier Silvestre. Relation of Silva de Peral & Alameda II: jump from n_ss to ns. Sent to: http://vixra.org/author/javier_silvestre

[7] Javier Silvestre. SPA III: Mc Flui transform for Silpovgar III and Silpovgar IV. Sent to: http://vixra.org/author/javier_silvestre

[8] Javier Silvestre. SPA IV: Silpovgar IV with Piepflui. Excess Relativistic: influence in LAN and SPA. Sent to: http://vixra.org/author/javier_silvestre

[9] Javier Silvestre. Feliz Theory of Eo vision - Relativistic II: influence in Riquelme de Gozy. Sent to: http://vixra.org/author/javier_silvestre

[10] Javier Silvestre. Pepliz LAN Empire I: $LAN_{n\to\infty}$ vs. LAN(P50). Sent to: http://vixra.org/author/javier_silvestre

[11] Kramida, A., Ralchenko, Yu., Reader, J., and NIST ASD team (2014). NIST Atomic Spectra Database (ver. 5.2.) [Online]. Available: http://physics.nist.gov/asd [2016, May 30]. National Institute of Standards and Technology, Gaithersburg, MD
[12] Kramida, A., Ralchenko, Yu., Reader, J., and NIST ASD Team (2015). *NIST Atomic Spectra Database* (ver. 5.3), [Online]. Available: http://physics.nist.gov/asd [2016, May 18]. National Institute of Standards and Technology, Gaithersburg, MD.
[13] https://dept.astro.lsa.umich.edu/

Abbreviations Table
Following Table indicates abbreviations used in this theory and its use in article in question is marked with X. 16, 17, 18 and 19 are [7] [8] [9] & [10] respectively. 20 is present article.

Abbreviation	**16**	**17**	**18**	**19**	**20**	**Meaning**
AC			X			Actual Change
AFEC	X	X				FEC adapted
BES						Born Electronic System
E_{dR}		X	X	X	X	Reference destiny energy
E_{dR}^{*}		X	X			Reference destiny energy with ER_{dR}
E_{dRI}			X			Ideal E_{dR} obtained from extrapolation of others E_{dR} satisfying Relation of Riquelme de Gozy
E_{jRI}						Ideal jump energy obtained from E_{dRI}
E_k	X	X		X	X	Reference Jump energy
$E_{k\text{-}SPA}$						E_k from LAN-SPA equality
E_o		X	X	X	X	1s OES Ionization energy
E_o^{*}		X	X			1s OES Ionization energy with ER_o
E_{oT}		X	X		X	1s theoretical ionization energy
EC						Energetic correlation in SPA
ER		X	X			Excess Relativistic
ER_{dR}		X	X	X	X	Excess Relativistic of E_{dR}
ER_o		X	X	X	X	Excess Relativistic of 1s ionization energy (E_o)
FEC	X	X				Fundamental Energetic Correlation
FPG			X	X	X	Relation of Flui Piep de Garberí
GLA					X	Global LAN_R amplitude
IE	X	X	X	X	X	Ionization energy
IE_G					X	IE Gozy method
JLA					X	Jump LAN_R amplitude
LAN	X	X	X	X	X	Serelles Secondary Lines Factor
LAN_M		X	X			LAN with modification
$LAN_{n\to\infty}$				X	X	LAN when $n\to\infty$
LAN_R*		X				LAN with reference data and considering ER
LAN_R	X	X	X	X	X	LAN with reference data

LAN_I LAN_{RI}						Ideal LAN obtained from E_d or E_{dRI}
LAN_S				X	X	LAN when $n=n_{START}=n_S$ and $E_k=0$
LAN(P50)		X		X	X	Initial LAN value in ns to ns jump. LAN with IE
LAN(P65)				X	X	Another denomination for $LAN_{n\to\infty}$
n	X	X	X	X	X	Principal quantum number
$n_{initial}$ or n_s	X	X	X	X	X	n of non-excited electron
OES						Origin Electronic System
PEC		X				Primitive energetic correlation of SPA
Piepflui		X				Constant spacing in Silpovgar IV
RC		X				Relative Change
RG			X	X	X	Relation of Riquelme de Gozy
SPA	X	X	X	X	X	Relation of Silva de Peral y Alameda
Z		X		X	X	Atomic Number
z_o			X	X	X	1s Origin charge according to P46
z_s		X	X	X	X	Start charge according to P46

ARTICLES INDEX

Part	Number	Title
Part I - Victoria Equation and Feliz Solutions	01	Victoria Equation - The dark side of the electron.
	02	Electronic extremes: orbital and spin (introduction)
	03	Relations between electronic extremes: Rotation time as probability and Feliz I.
	04	Feliz II the prudent: Probability radial closure with high order variable C_F
	05	Feliz III The King Major: Orbital filled keeping Probability electronic distribution.
	06	Feliz IV Planet Coupling: Probability curves NIN coupling from origin electron.
	07	NIN Coupling values in n=2 and Oxygen electronic density.
	08	Electron Probability with NIN coupling in n=2.
	09	Electron probability with NIN coupling in n>2 and necessary NIN relationships.

Part II – Excited electron: Tete Vic and LAN	10	Excited electrons by Torrebotana Central Line: Tete Vic Equation.
	11	Excited electrons: LAN plains for Tete Vic Equation.
	12	Relation of Riquelme de Gozy: LAN linearity with energy of excited states.
	13	Relation of Fly Piep de Garberí: LAN^{-1} and Ionization Energy.
	14	Relation of Silva de Peral & Alameda: LAN interatomicity with energetic relation.
	15	Relation of Silva de Peral & Alameda II: jump from n_ss to ns.
	16	SPA III: Mc Flui transform for Silpovgar III and Silpovgar IV.
	17	SPA IV: Silpovgar IV with Piepflui. Excess Relativistic: influence in LAN and SPA
	18	Feliz Theory of Eo vision - Relativistic II: influence in Riquelme de Gozy
	19	Pepliz LAN Empire I: $LAN_{n\to\infty}$ vs. LAN(P50)
	20	Pepliz LAN Empire II: $LAN_{n\to\infty}$ vs. LAN(P50)
Part III - NIN: C_{PEP} & C_{POTI}	21	Electron Probability: PUB C_{PEP} I (Probability Union Between C_{PEP}) - Necessary NIN relationships
	22	Electron Probability: PUB C_{PEP} II in "Flui BAR" (Flui (BES A (Global Advance) Region)
	23	Orbital capacity by advancement of numbers - Electron Probability: PUB C_{PEP} III: "Flui BAR" II and $C_{PEP\text{-}i}$
	24	Electron Probability: 1s electron birth: The last diligence to Poti Rock & Snow Hill Victoria
24 hours of new day		